31.05.2023

High-dimensional Characterisation of rare cerebrospinal fluid cells in relapsing remitting multiple sclerosis patients

Håkon Olsen

Thesis for the degree of Master of Science in Medical Biology

Department of Biomedicine &
Department of Clinical Medicine at the University of Bergen, Norway

UNIVERSITY OF BERGEN
Håkon Olsen

Acknowledgements

Firstly, I would like to express my profound gratitude to my supervisors Sonia Gavasso, Shamundeeswari Anandan, and Kristina Xiao Liang for giving me guidance, training and fantastic help throughout the process. This project would not have started without all your ideas and input. Shamundeeswari, your technical knowledge and skills was of immense help in the laboratory and with problem solving during the project. Sonia, your expansive knowledge in the field and resourcefulness was crucial for optimisation and problem solving when i encountered problems. Xiao, thank you for all the training in the cell lab and sharing your knowledge of the stem cell field. I have fully enjoyed working with all of you during this project and would like to thank you all again for the help and feedback you have all provided me with.

I would like to thank Jørn Skavland and the rest of the Flow Cytometry Core Facility for training, and technical support with the IMC experiments.

In my office micro-environment, I would like to thank my fellow students, Bjørn, and Yola for continued emotional and mental support throughout the project. Both when my project was going well and when it was going slow. Sharing an office with you both in this research period has been a great experience.

I would like to give thanks to my family, for pushing me to find a passion for research, and the unconditional love they have shown me even while living hundreds of miles away. The rest of my friends both in Bergen and other parts of the country for the support they have shown me, and for pushing me to spend more time on my hobbies outside of my work. Lastly, I would like to thank my best friend and partner, Léa. Your passion makes me smile and you truly make my life happier.

Table of contents

Abbreviations

BBB – Blood-brain barrier

BCSFB – Blood-CSF barrier

BM – Bone marrow

c-Myc – Cellular myelocytomatosis oncogene

CNS – Central nervous system

CSF – Cerebrospinal fluid

CP – Choroid plexus

DPBS – Dulbecco's phosphate-buffered saline

ESCs – Embryonic stem cells

HIV – Human Immunodeficiency Virus

IBA1 - Ionized calcium binding adaptor molecule 1

IGF-1 – Insulin-like growth factor 1

IF – Immunofluorescent

IMC – Imaging mass cytometry

iPSCs – induced pluripotent stem cells

iPSC-MG – iPSC-derived microglia

Klf4 – Krüppel-like factor 4

LIF – Leukaemia inhibitory factor

Lin28 – Protein lin-28 homolog A

MEF - Mouse embryonic fibroblasts

MOG – anti-myelin oligodendrocyte glycoprotein

MRI – Magnetic resonance imaging

MS – Multiple sclerosis

NANOG – Nanog Homeobox

NSPCs – Neural stem/precursor cells

NTSCs – Nuclear transfer stem cells

Oct3/4 – Octamer-binding transcription factor 3/4

P2Y12 - P2Y purinoceptor 12

PBMCs – Peripheral blood mononuclear cells

PBS - Phosphate-buffered saline

PET – Positron emission tomography

PPMS – Primary progressive multiple sclerosis

PSCs – Pluripotent stem cells

RRMS – Relapsing remitting multiple sclerosis

RT – Room temperature

SMC – Suspension mass cytometry

Sox2 – SRY box-containing gene 2

SPMS – Secondary progressive multiple sclerosis

TMEM119 - transmembrane protein 119

TNF – Tumour necrosis factor

VSELs – Very small embryonic-like stem cells

Summary

Multiple Sclerosis (MS) is a chronic inflammatory and neurodegenerative disease of the central nervous system (CNS) and is the leading cause of neurological disability in young adults in North America and Europe, affecting approximately 2.5 million people worldwide. The pathological features associated with MS include neurodegeneration and brain atrophy, axonal loss, cortical demyelination, microglia activation, and a failure of remyelination. The cerebrospinal fluid (CSF) is referred to as the "mirror of the brain", and recent studies have shown that biomarkers reflecting inflammation and the stages of MS can be found in the CSF. The CSF contains immune cells, especially under pathological conditions.

Recent studies have observed microglia cells in the CSF of individuals with relapsing remitting MS using single cell RNA sequencing. The study showed evidence that microglia of individuals with relapsing remitting MS may have the capability to migrate from the central nervous system into the CSF. Microglia are the resident macrophage of the central nervous system and are intricately bound to mechanics of neurological diseases by producing both neuroprotective and neurotoxic effects depending on stimuli. Characterising CSF cells and particularly microglia in depth is challenging and advances in new technologies allow to phenotype these cells at unprecedented resolution.

We aimed at characterising the immune cells in CSF of relapsing MS patients in detail. By utilizing our groups expertise with Imaging mass cytometry, we developed and optimised a protocol for capture and analysis of CSF cells from single cell suspension. For this protocol an imaging mass cytometry panel of metal conjugated antibodies was developed for high-dimensional immunophenotypic analysis of microglia. Focusing on microglial cells, we possibly detected these cells in CSF and performed analysis using specific microglial markers and general immune markers. The analysis was performed alongside controls for characterisation, iPSCs-derived microglia, a commercial microglia cell line, PBMCs and buffy coats.

Our results show the expression of various immune and microglia markers in cells of the CNS and controls. The iPSCs derived microglia and commercial cell line showed distinct expression of microglia markers and the same markers were detected in CSF cells of MS indicating that microglia may in fact be detected in CSF. Not all antibodies worked, and techniques need further optimisation for detections of both immune cells and microglia.

The procedure we developed shows great potential to analyse CSF cells and needs further optimisation in order to characterise and distinguish neuroprotective and neurotoxic microglial cells in the CSF. The approach developed in this thesis will expand the understanding of the central nervous system immune architecture in relapsing MS patients.

1. Introduction

1.1 Multiple Sclerosis

MS is a chronic inflammatory, demyelinating, and neurodegenerative disease of the CNS of presumed autoimmune aetiology. MS is a heterogenous, multifactorial, immune-mediated disease that is caused by complex gene-environment interactions. Recently, compelling evidence has shown that MS is a rare complication of a common infection with Epstein-Barr Virus (EBV) but mechanisms of progression remain elusive (1). The disease gives rise to focal lesions in the grey and white matter and to diffuse neurodegeneration in the entire CNS and it is the leading cause of neurological disability in young adults in North America and Europe affecting approximately 2.5 million people worldwide (2, 3, 4, 5). Clinical symptoms of the disease are various and include sensory and visual disturbances, motor impairment, fatigue, pain, and cognitive deficits. The variation of clinical symptoms correlate with the spatiotemporal spread of the lesions in the CNS (5, 6, 7). The lesions are the main hallmark of MS, and they are caused by immune cell infiltration across the blood-brain barrier (BBB), which is broken down in the pathological process of the disease, and these immune cells promote inflammation, demyelination, gliosis and neuroaxonal degeneration (3, 5). While the lesions are the main hallmark of MS, the immune-mediated destruction of CNS myelin and oligodendrocytes are considered the primary pathology of MS and the progressive axonal loss the major cause of neurological disability in MS (6). The disease is presumed to be autoimmune since studies have observed emergence of T cells early in lesion formation. The activation of peripheral autoreactive effector CD4 T cells which migrate into the CNS may initiate the disease process, this hypothesis is known as the “outside-in hypothesis”. This model fits well with molecular mimicry proposed between EBV and CNS GlialCAM

epitopes. The opposing hypothesis is the “inside-out hypothesis”, where MS may be triggered by an initial event in the CNS, such as persistent inflammation or a viral infection (3, 4, 5).

The course of the disease does not manifest identically in all patients and thus has been divided into three clinically distinct subgroups by prevalence and severity. From highest prevalence to lowest these are: relapsing remitting multiple sclerosis (RRMS), secondary progressive multiple sclerosis (SPMS), and primary progressive multiple sclerosis (PPMS). Approximately 85% of MS patients have RRMS, which is classified by a disease course that alternates between episodes of inflammation and neurodegeneration, and episodes of recovery. This alternating course can last for many years and these RRMS patients benefit from highly effective immune modulating drugs (6, 8). Unfortunately, approximated 90% of patients with RRMS transform into SPMS, gradually over years, and SPMS is classified by a steady neurological decline without immune attacks (6). PPMS is observed in about 10% of MS patients at onset, and the course is characterised by steadily increasing neurodegeneration without immune attacks and recovery periods (6). The pathological features associated with progressive MS include neurodegeneration and brain atrophy, related to axonal loss, cortical demyelination, microglia activation, and a failure of remyelination (3). A diagram representing the difference in disease subgroups alongside a “benign” course of MS is shown in Figure 1.

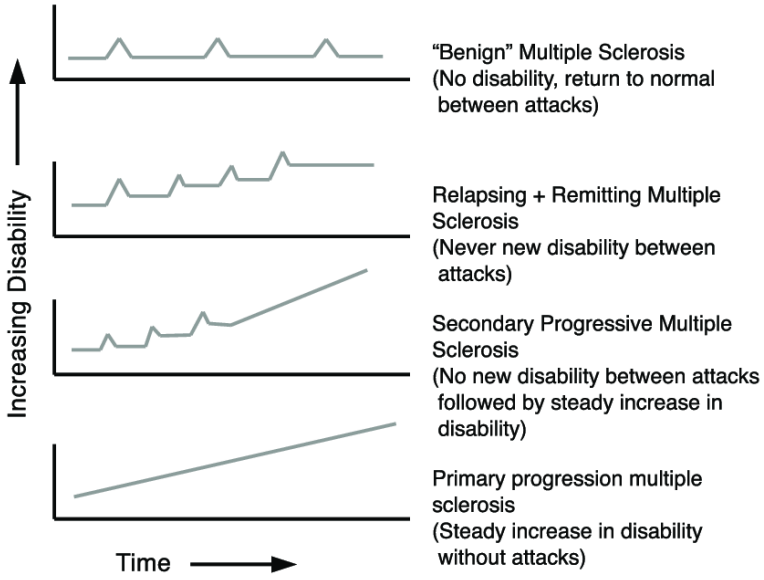

***Figure 1**: Diagram showing the different types of MS with increasing disability over time(9). The peaks represents attacks and recovery phases. Note that only benign MS shows complete recovery after attacks while all other forms of MS show a steady worsening of disability over time.*

RRMS involves trafficking of immune cells from the periphery into the CNS, whereas progressive MS involves the development of a compartmentalised pathological process within the brain (3). An illustration of the mechanisms of progressive MS is shown in Figure 2.

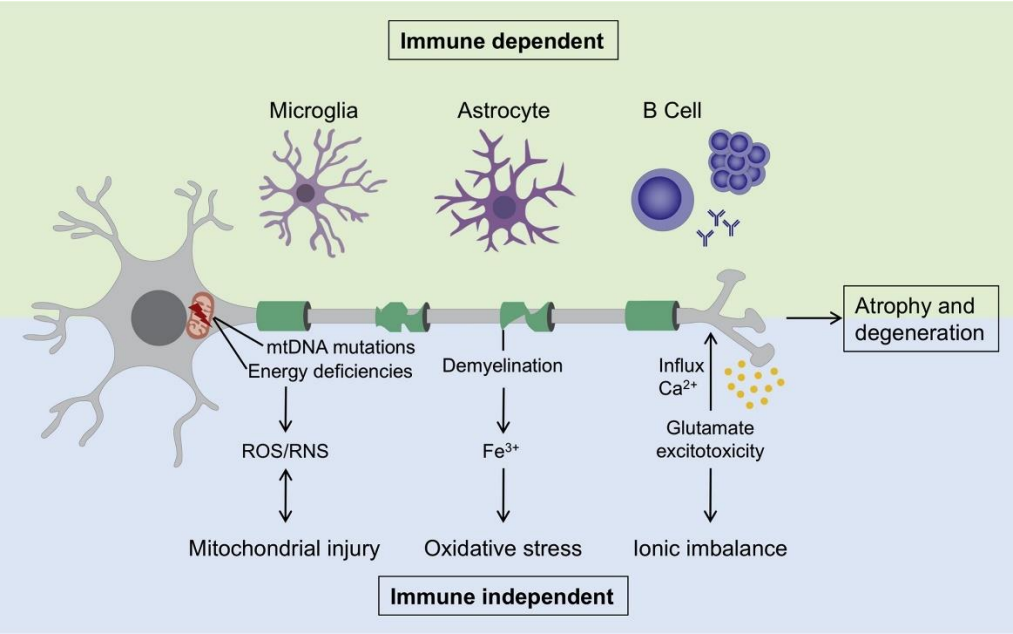

Figure 2: *Mechanisms of progressive multiple sclerosis. CNS resident immune cells, including microglia, astrocytes and B cells can drive the neurodegenerative processes in progressive MS. The immune-dependent components of the disease can activate various disease processes that then become self-maintaining and immune-independent, such as mitochondrial injury as a result of mitochondrial DNA mutation and enhanced production of reactive oxygen species, oxidative stress occurring from iron release from active demyelination areas, and ionic imbalance stemming from glutamate excitotoxicity which causes a massive influx of calcium into neurons. All these mechanisms lead to axonal atrophy and neurodegeneration (10).*

Currently, the immunomodulatory therapies for MS decrease immune mediated damages to the CNS. It has been suggested that autoimmune response-instigated neuroaxonal injury triggers a potentially self-sustaining chronic neurodegenerative process (5, 6). This process progresses even in the absence of new immune cell infiltration from the periphery. A possible explanation for the immune cell infiltration decrease is the reduction in the breakdown of the BBB and immune cell exhaustion associated with chronic antigenic exposure (3, 5). The infiltrating immune cells contribute to the early phases of inflammation in MS, and activate CNS-resident cells, mainly microglia and astrocytes. These CNS-resident cells can sense homeostatic disturbances and generate a range of neurotoxic inflammatory cytokines, chemokines, and reactive oxygen species, that promote and sustain neuroaxonal damage and thus neurodegeneration both in the early stages and later stages of the disease (5). Microglia in particular have a range of functions in the CNS and are the resident CNS macrophage. An introduction to microglia is presented in section 1.3.

With MS being a disease of the CNS, studying it poses challenges. Brain biopsy, for example, are extremely invasive and can have devastating consequences, and ethical implications. Research of patients living with the disease has then focused on other brain imaging techniques, such as positron emission tomography (PET) scans, and MRI scans to visualise the lesion formation and development in the brain. In biomarker discovery and immunological studies, research has focused on the two liquids found in the CNS, the blood, and the CSF. The blood which is relatively easily collected and biobanked has been extensively used in MS research. Studies in CSF, however, pose some specific challenges, such as an extremely limited cell concentration and collection procedures being more invasive than blood. The CSF contains immune cells, especially under pathological conditions such as MS, but these are rare and biobanking analysis of CSF cells is a challenge. The CSF is referred to as the "mirror of the brain", and recent studies have shown that biomarkers reflecting inflammation and the stages of MS can be found in the CSF such as neurofilament light chain. To elucidate MS disease mechanism and enhance biomarker discovery studying the CSF, as the mirror of the brain, is essential. Specifically, developing robust techniques that allow deep characterisation of cells in the CSF as the single cell level are of great interest in neurological diseases. Imaging mass cytometry, discussed in section 1.5 of the thesis, is a promising tool for unprecedented immune phenotyping of rare cells in the CSF and the development of such a procedure is an aim for this thesis.

1.2 Cerebrospinal fluid

CSF is a clear, colourless liquid that surrounds the brain and spinal cord. One important function is to cushion the brain within the skull, serving as a shock absorber for the CNS tissue. Additionally, the CSF is crucial in maintaining a healthy functional environment in the CNS by circulating nutrients and chemicals filtered from the blood, transporting vitamins, growth factors and proteins into the CNS through the blood-CSF barrier (BCSFB) and by removing harmful metabolites from the CNS (11, 12). In recent studies it has been shown that the CSF, beside serving as a shock absorber and circulatory fluid, has multiple other crucial functions for the CNS throughout the life of the organism, actively engaging in development, homeostasis, and repair of the CNS. The choroid plexus (CP), for example, where the CSF is produced, also synthesizes trophic and angiogenic factors, chemorepellents, and carrier proteins, which it supplies to the CNS (12). The functions that the CSF and the CP are responsible for or contribute to are many and complex and are of prime importance in both MS and healthy individuals.

CSF is important in neurological diseases such as MS because it is the body fluid closely reflecting the pathology of MS. Many, biomarkers relating to the disease are first discovered in the CSF, the “mirror of the brain”. For example, IgG bands in CSF are used in MS diagnostic and therapy monitoring, and Neurofilament light chain discovered first in CSF is a biomarker for neurodegeneration not only in MS but also in other neurological diseases. The discovery of meaningful biomarkers in the CSF is an ongoing research effort in MS, because, reliable, functional biomarkers can be of use in multiple areas, potentially providing an early diagnosis, better prognosis of the disease course and influencing the choice of therapy for individual patients, and monitoring the therapy response and potential side-effects (13, 14, 15). For the study of cells in CSF, one technical challenge is the low number of immune cells, with a cell concentration of 1-5 cells/µl in healthy individuals. MS patients have a higher cell concentration in the CSF partly caused by inflammation and breakdown of the BBB allowing for migration of immune cells into the CSF, and the concentration of cells in the CSF is about 5-50 cells/µl (13, 16). A figure showing the presence of immune cells and other cell types that are inflammatory markers in the CSF mirroring the inflammation of the CNS is shown in Figure 3.

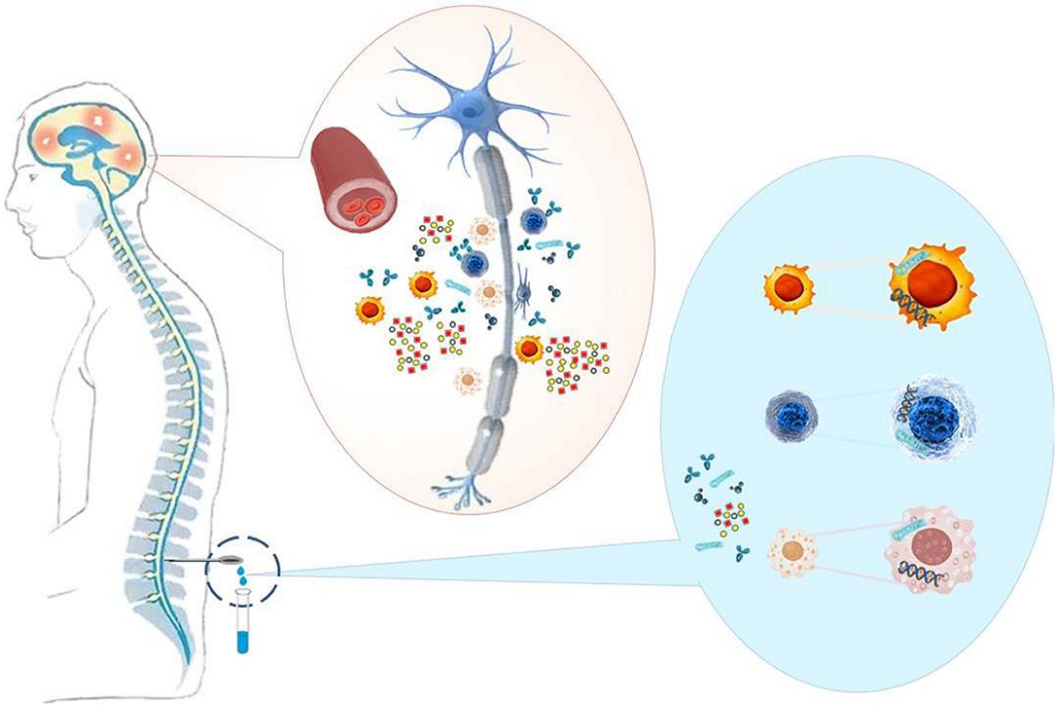

Figure 3: *Figure showing the presence of immune cells, pathological antibodies, adhesion molecules, cytokines, chemokines and nucleic acids in the CSF which reflects inflammation in the CNS in MS patients. some of these cells are intrathecal immunoglobins, leukocytes, lymphocytes, CXCL13, IL6, IL8 and IL10(17).*

In a recent novel study of CSF in people with virologically suppressed Human Immunodeficiency Virus (HIV), using single-cell RNA-sequencing, a novel myeloid subset

was identified, with gene expression characteristics of neurodegenerative disease-associated microglia (18). This study to our knowledge is the first to identify circulating microglia-like cells, adding them to the list of inflammatory markers in the CSF that reflect the inflammation of the CNS. These microglia-like cells are very rare, according to the study they represent <5% of all the cells they analysed in the CSF (18). In the study they showed that the HIV positive individuals had a higher frequency of the microglia-like cells than the control individuals, thus the authors suggested a potential link between the presence of the microglia-like cells and chronic immune activation in the CNS during HIV infection (18).

Similarly, another study showed that Microglia-like cells are present in the CSF of RRMS patients. This study used single-cell RNA sequencing on CSF cells from individuals with RRMS and anti-myelin oligodendrocyte glycoprotein (MOG) disorder, and confirmed the findings of the previous study, by focusing on CSF myeloid cell types, they identified microglia in human CSF with a gene expression profile of parenchymal microglia (16). The presence of Microglia like cells in the CSF suggests that the microglia of individuals with MS, specifically RRMS, have the capability to migrate from the CNS into the CSF over the course of the disease. The study doesn't show how the CSF microglia gain access to the CSF, but the authors theorize that they might traverse the pia mater or choroid plexus, or traffic into the CSF through perivascular spaces or via lymphatic drainage. They do find some support for the hypothesis that the migration occurs in response to chemokines as they found chemokine receptors on the cells, including CCR1, CCR5, CXCR4, and CX3CR1 (16).

The possible presence of microglial cells in CSF of RRMS patients, and the possibility that they may contribute to the MS disease progression such as inflammation, neurodegeneration and neuro-regeneration in unexpected ways, warrants further investigation into this topic, an aim for this thesis.

1.3 Microglia

Microglial cells are the resident tissue macrophage in the CNS, including the brain, the retina and the olfactory bulb, and they are primary innate immune cells. In the CNS of adult mice, they account for approximately 10% of the cell population, and their estimated number in the CNS is 3.5 million (19, 20, 21, 22). The number of microglial cells in the adult human brain depends on the anatomical region, and thus, depending on the brain region, they account for 0.5-16.6% of the total cell population in the brain (23). Microglia play a central role in early CNS development and sustain homeostasis in adults and interestingly it's been shown in

recent findings that they take up residence in the developing brain before the differentiation of other CNS cell types, which is probably because they are critical regulators of CNS development (19, 24, 25, 26). In addition, microglia also regulate the BBB together with endothelial cells (ECs), pericytes and astrocytes. The BBB is a specialized endothelial structure mainly comprised of ECs and pericytes that selectively separate the sensitive brain parenchyma from blood circulation (27, 28).

Microglia are of myeloid lineage, originate in the embryonic yolk sac from specialised precursor yolk sac macrophages, and migrate into the developing CNS before the BBB is fully developed (29, 30). The Microglia are one of the first tissue macrophages to develop in the yolk sac, and it's been shown in mice models that they are distinct from other tissue macrophages by the expression of the transcription factor PU.1 (29, 31). The migration of microglia into the CNS occurs before the differentiation of other resident nervous system cells, such as astrocytes and oligodendrocytes (19).

Recent studies have showed that microglia persist throughout the entire life of the organism without input from circulating blood cells. Studies in mice using bone marrow (BM) irradiation and chimerism have shown that, under physiological conditions, circulating monocytes do not contribute to the adult microglia pool and that the expansion potential of the microglia in the CNS is sufficient to provide enough progeny for the lifetime of the organism, both under physiological conditions, and during disease (24, 31, 32).

There is an extensive number of different tasks that the microglia perform or contribute to during both the development of the CNS and in the fully mature CNS. These include: elimination of apoptotic cells and preventing an oversupply of neurons, support of neurogenesis, migration and differentiation of neurons, axon growth and synaptogenesis, immune surveillance, injury response, generation and maturation of astrocytes and oligodendrocytes and angiogenesis (24). A figure showing an overview of the many tasks microglia perform and contribute to in the developing and mature CNS is shown in Figure 4.

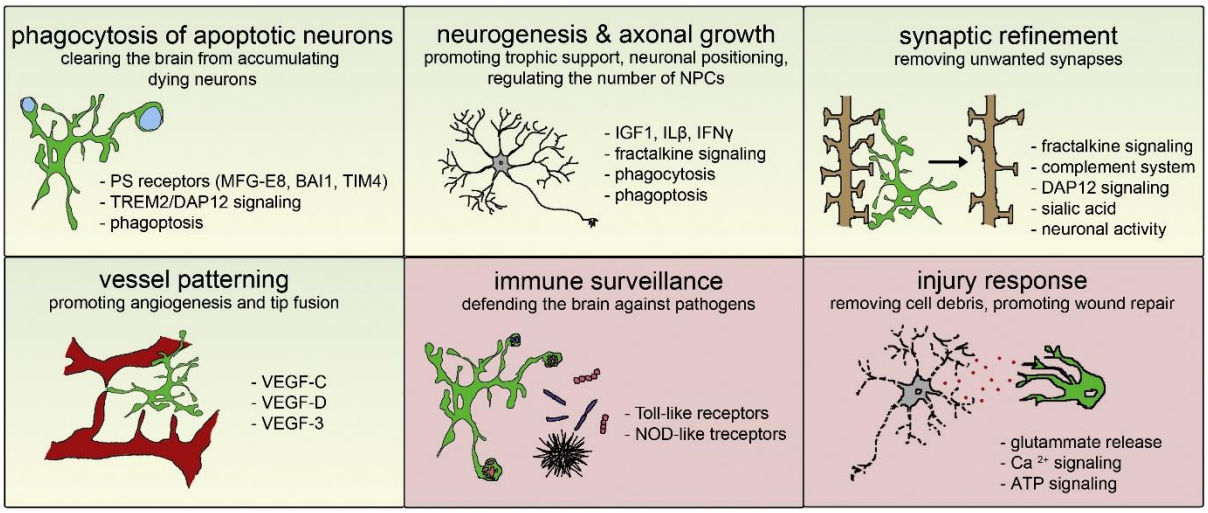

Figure 4: *An overview of the many functions' microglia perform in the developing CNS and in the mature CNS. The figures with a blue background show functions in developing CNS, while figures with a pink background show functions in the mature CNS (33).*

In the developing CNS, various neurotrophic factors promote survival and differentiation of neuronal cells alongside synaptogenesis, and microglia contribute by releasing trophic factors that support the formation of neuronal circuits and promote their survival. One example of this is the release of insulin-like growth factor 1 (IGF-1) by microglia, which promotes the survival of cortical neurons during postnatal development (30).

During brain development immature neurons and other resident cells are born and migrate to their appropriate location, and a subset of these cells must be killed off by programmed cell death so that the rest can mature. In fact, the number of immature neurons that are killed off in this process is approximately half. The immature neurons that are killed are usually results of defective differentiation or have failed to form proper neuronal circuits (19, 25, 30). Microglia are attracted to and accumulate in areas with high densities of apoptotic neurons, where they engulf these cells and facilitates phagocytosis without triggering an inflammatory response and thus facilitate neuronal turnover in the organism. In addition to clearance of dead cells, the phagocytic activity of microglia is crucial for synaptic homeostasis, with microglia participating in neuronal pruning, and responding to synaptic activity as well as plasticity, as proper synaptic function depends on various trophic factors and synaptogenic signals, which are expressed by microglia (25, 30).

In addition to neurons, microglia have been implicated in the development of other resident CNS cell types, such as astrocytes and oligodendrocytes. For example, microglia-conditioned media increases the differentiation of neural stem cells/precursor cells (NSPCs) into astrocytes through Il-6 and leukaemia inhibitory factor (LIF), and microglia-conditioned

media promotes the survival and differentiation of cultured oligodendrocyte precursor cells into mature oligodendrocytes through secreted factors including IGF-1, nuclear factor kappaB, IL-1β, and Il-6 (25, 34, 35).

Microglia are involved in and are responsible for many functions in the CNS, both in the developing and mature brain. However, the study of microglia biology in MS remains a challenge and studies are primarily based on post-mortem tissue. In MS, increases in microglia activation has been observed both in lesions and in normal-appearing white matter (5). Microglia can produce a range of neurotoxic inflammatory mediators. Some of the different inflammatory and oxidative stress mediators that activated microglia secrete in MS are the cytokines tumour necrosis factor (TNF), IL-1b, and IL-6, the chemokines, macrophage inflammatory protein MIP-1a, monocyte chemoattractant protein, MCP-1, and interferon inducible protein IP-10 (36, 37). These neurodegenerative and inflammatory mediators are observed in the inflammatory state of MS, while the neurodegenerative processes in the chronic state of MS are dominated by neuron loss resulting from oxidative stress and excitotoxicity (5, 6). The oxidative burst in activated microglia and macrophages is regarded as the major source of reactive oxygen species in MS (37). Recent data showing that activated microglia produce reactive oxygen species and nitrogen oxide radicals in MS lesions, further expand their role in the demyelination and neurodegeneration of MS (38, 39).

Interestingly, evidence also shows microglia participating in the remyelination process in the brain, in addition to the neurodegenerative processes leading to demyelination. In the remyelination process two key parts of the process are debris clearance and proliferation of oligodendrocytes, in which microglia plays a major role. During the initiation process of remyelination the phagocytosis of myelin debris plays an important role, and is performed by macrophages and microglia (40). Furthermore, a study in 2015 found that CX3CR1 knockout mice had an impaired remyelination and reduced myelin debris clearance due to reduced function of microglia, clarifying its importance in the process (41). Further, microglia produce factors that are important to the differentiation of oligodendrocyte precursors into mature oligodendrocytes. A recent study found that the production of TNF-α, IGF-1 and fibroblast growth factor 2 (FGF-2) by microglia is very important to the proliferation of oligodendrocytes and creates an environment promoting regeneration (42).

With the vital functions of microglia in health and MS and confirmed observations of the cell type in the CSF, we aim to characterise these cells in depth with imaging mass cytometry and

for example determine whether the microglia found in the CSF of MS patients are neurotoxic or neuroprotective.

1.4 Induced pluripotent stem cells

Pluripotent stem cells are characterized by their properties of self-renewal and potency, where self-renewal refers to the cell's ability to proliferate and potency refers to the cell's ability to differentiate into specialized cell types derived from one of three primary germ layers, namely, ectoderm, endoderm, and mesoderm (43). Pluripotent stem cells are further designated into four different types, naturally occurring Embryonic stem cells (ESCs), and,- Very small embryonic-like stem cells (VSESLs), and technically derived Induced pluripotent stem cells (iPSCs), and Nuclear transfer stem cells (NTSCs) (43). There is one other type of stem cell as well, adult stem cells, but this type of stem cell is not pluripotent unless reprogrammed into a naïve state (43). This lack of pluripotency does not remove their clinical utility, specifically in cell therapy, but it does limit their use into niches based on the specific organ the cells are harvested from.

Among different types of the pluripotent stem cells, iPSCs have shown several advantages that make them a promising avenue for research and potential therapies. Unlike ESCs, the creation of iPSCs does not involve the destruction of an embryo, thus circumventing a major ethical issue associated with ESCs. Since iPSCs can be derived from the patient's own cells, they can potentially be used to create personalised therapies. This reduced the risk of immune rejection, which is a common complication with non-autologous transplants.

In 2006 it was shown that iPSCs could be generated from mouse embryonic fibroblasts (MEF) by the retrovirus-mediated transfection of four transcription factors, specifically octamer-binding transcription factor 3/4 (Oct3/4), SRY box-containing gene 2 (Sox2), Cellular myelocytomatosis oncogene (c-Myc), and Krüppel-like factor 4 (Klf4) (44). It has further been shown that iPSCs can be generated from adult human dermal fibroblasts using the same transcription factors (44), these iPSCs can also be generated from other types of somatic tissues, such as blood, skin, and urine (43). In addition, they show promise for drug discovery and personalized medicine due to their patient source and that they carry the generic patient background, thus avoiding immune rejection when transplanted autologously (43).

Deciphering the specific mechanisms by which pluripotency is induced in somatic cells is an ongoing research topic in stem cell research, and decent progress has been made since the

first documentation of reprogramming stem cells into iPSCs using Oct3/4, Sox2, C-Myc, and Klf4. Of the four factors, Oct3/4 & Sox2 have been shown to be essential in the generation of iPSCs and maintaining pluripotency while c-Myc and Klf4 are important because c-Myc & Klf4 may induce global histone acetylation, which allows Oct3/4 and Sox2 to bind to their specific target sites (45). C-Myc has many downstream binding targets that enhance transformation and proliferation, however overexpression of C-Myc has been shown to induce differentiation and apoptosis of human stem cells (44, 45). Considering this, the role of Klf4, in relation to reprogramming, becomes easier to postulate as Klf4 has been shown to repress p53 directly and thus might function as an inhibitor of Myc-induced apoptosis through the repression of p53. While being an inhibitor of p53, Klf4 also activates p21, and thus supressing cell proliferation, this function of Klf4 might be inhibited by c-Myc, which suppresses the expression of p21 (44, 45). From their functions, we can deduce that the balance of Klf4 and c-Myc may be vitally important for generation of iPSCs when using the original transcription factors in the reprogramming process. The four original transcription factors are not the only ones that can be used in the reprogramming process. In newer years it has been shown that Klf4 and c-Myc can be replaced by other transcription factors, with specifically Nanog Homeobox (NANOG) and Protein lin-28 homolog A (Lin28) being effective substitutes. The modified induction protocol using Oct4, Sox2, NANOG, and Lin28 showed an efficacy similar to the original induction protocol (43). Currently the use of different transcription factors in reprogramming seems to have differing efficiency for producing specific cell subtypes in various stages of maturity and as such this is an ongoing inquiry in the stem cell research field (43). The search for other transcription factors in reprogramming, and induction methods requiring fewer transcription factors are two other ongoing major inquiries in the field.

A protocol for the generation of microglia from human derived iPSCs with reliable reproducibility was published in 2017. This protocol generated iPSC-derived microglia (iPSC-MG) and showed that they resembled primary human microglia in morphology, gene expression, and cytokine release, while differing from other tissue macrophages (46). The iPSC-MG generated by this method expressed the known microglia markers Ionized calcium binding adaptor module (IBA1), CD11c, transmembrane protein 119 (TMEM119), P2Y purinoceptor 12 (P2Y12), CD11b, and CX3CR1, and their expression levels were compared with those of foetal human primary microglia (46). The promising data of the method presented in the paper is a tool to differentiate microglia from MS patients that can be used in

complex *in-vitro* models such as organoids and tissue-on-chips to study intricate cell interaction in MS. In our study we aim at differentiating human microglia for in depth characterisation of markers that could be used in CSF cell studies.

1.5 Imaging mass cytometry

Imaging mass cytometry (IMC-Hyperion) is a technique that enables high multiplex imaging of cells or tissue by staining them with rare heavy metal-conjugated antibodies. It is capable of both detecting and visualising up to 40 different markers, with minimal cross-talk, simultaneously, and has become a powerful tool in the study of complex tissue morphology (47). The technique was first developed in 2014 as a complimentary method to suspension mass cytometry (SMC), by adding an additional platform for ultra-violet laser ablation (Hyperion Tissue Imager, Standard BioTools, San Francisco, USA) and giving the spatial resolution of the data obtained (47, 48). In the field of imaging techniques it is a major leap forward as standard immunofluorescence imaging methods are limited to a maximum of 5-7 different fluorophore-conjugated antibodies due to emission overlap, while the high-precision of the Hyperion comes from the fact that the metals in the conjugated antibodies are being detected by mass, as the detection is performed in the time-of-flight mass spectrometer, an integral part of the machine (47). This high precision has allowed the Hyperion to detect up to 40 different markers, with the possibilities of expansion to potentially 100 different markers as isolation of rare metals continue and become available for antibody conjugation (48). Data acquisition of IMC data is relatively simpler compared to the data analysis, due to the high dimensionality of the IMC data it is difficult to comprehend the complexity of the images just by visually evaluating staining patterns (47). A schematic overview of a general IMC workflow is shown in Figure 5 below.

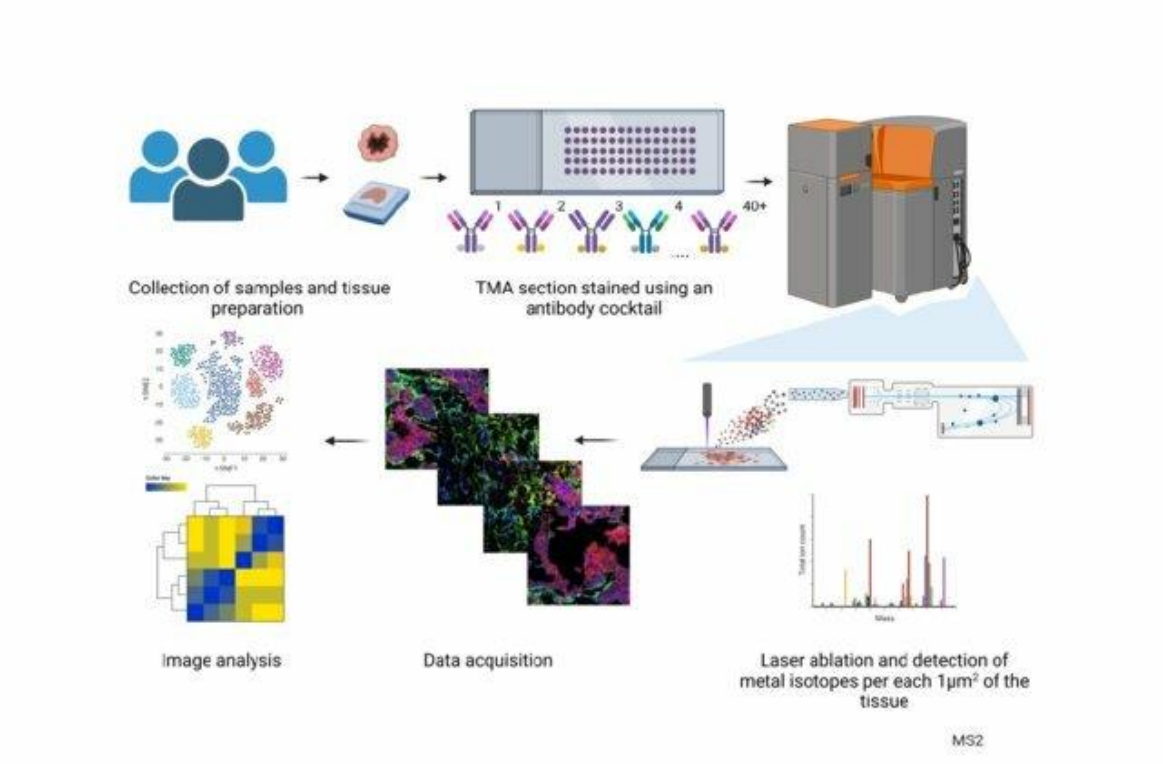

Figure 5: *A schematic overview of a general Imaging Mass Cytometry workflow. Tissue samples are first collected, then stained with an cocktail of metal isotope-coupled antibodies. Dried and stained tissues are loaded into the ablation chamber of the Hyperion tissue imager, where stained tissues are ablated by a stationary UV light beam 1μm^2 at a time. By each ablation cycle, 1μm^2 of the tissue is evaporated, creating plumes of tissue and antibody residues, and metal isotopes. The plumes are carried by argon gas into the CyToF mass spectrometer, where the time of flight is measured for each 1μm^2 of tissue, detecting the specific metal isotopes and their position on the grid, allowing the presence and position of each of the markers to be reconstructed creating a digital pseudo image of the tissue which is then used in image analysis (49).*

The Hyperion imaging mass cytometry technology is integral to our work in this thesis. Our group has extensive knowledge in the field, and we have established microglia 40 marker panels for imaging tissue. The Hyperion tissue workflow needs to be adapted to CSF cells on slides. With this optimized technique in place, we will characterize the cells in the CSF of RRMS patients focusing on microglia cells and immune cells. In addition, we will differentiate our own microglial cells from iPSCs, to further characterise differences in marker expression between the microglia found in the CSF and the microglia developed from healthy controls.

2. Aims

The overall aim of this study is to characterise the CSF immune cells in detail, for improved understanding of the CNS immune architecture in relapsing MS patients.

Firstly, we aim to characterize cells in the CSF of RRMS patients at unprecedented single-cell resolution by customizing our IMC (Hyperion) pipeline. Secondly, we aim to develop

quality controls for precise identification and detection of the unique microglial cells and immune cells within the CSF samples. Thirdly, we aim to quantify the difference in expression markers between microglia cells found in CSF of RRMS patients and microglia from other neurological diseases and healthy controls.

3. Materials and methods

3.1 Cell Culture and differentiation of microglial cells

3.1.1 iPSC culture

The iPSC lines were previously generated from a collaboration with Gareth Sullivan, UiO. Detroit 551 (ATCC® CCL-110™) fibroblasts were reprogrammed by overexpression of the transcription factors Oct4, Sox2, c-Myc and Klf4 as described previously (50). All the iPSC cells and research were approved by the Ethical committee (REK 2012/919). All the cell culture procedures were carried out under sterile conditions in a laminar flow hood. All cell lines were routinely checked for mycoplasma contamination using the MycoAlert™ assay kit (Lonza, cat#LT07-318). For the maintenance of iPSCs feeder-free protocols were used and the feeding, culturing, splitting, and thawing was performed as follows.

3.1.2 Feeding iPSCs

The tissue-cultured treated 6-well plates were coated with 1x Geltrex (Gibco™) solution by diluting the Geltrex 100x (Gibco™, cat#A1413201) with Advanced DMEM (Gibco™, cat#12634010). Geltrex is a synthetic basement membrane, acting as a substrate for cell adhesion. The Geltrex solution was kept at 4°C to avoid gelling. After adding 1 ml of the Geltrex solution to each well, the plates were incubated at 37^{O}C, 5% CO_2 for at least 45 minutes. The solution was aspirated before plating the cells. The iPSCs were observed and fed daily with 2 ml Essential E8 medium (E8 medium, Gibco™, cat#A1517001), which was made by combining the basal medium with the supplement provided in the kit. The medium was always equilibrated to room temperature (RT) before feeding the cells, and the old medium was completely aspirated before adding the new medium. The plates were kept in a humified incubator with a temperature of 37^{O}C and 5% CO_2.

3.1.3 Splitting iPSCs

When the cells reached approximately 60-70% confluency, they were split 1:2 into new plates. The old medium was aspirated from the cells, and Dulbecco's phosphate-buffered saline (DPBS) -/- (without calcium and magnesium, Gibco™, cat#14190250) was used to carefully wash the cells. 1 ml EDTA solution (0.5mM EDTA in DPBS) was added to each

well to detach the cells and the cells were incubated at 37^{O}C 5% CO_2 for 5 minutes. The EDTA was aspirated and 4 ml of complete E8 medium was added to each well with high force using a 10-ml pipette with a quick hand motion. The hand motion while releasing the medium should optimally cover the whole area of the well, without hitting any spots of cells twice. This is to ensure even size of the cell colonies, preventing them from becoming too small or big. The cell suspensions were distributed to new Geltrex coated wells, by adding 2 ml to each well. Before placement into the incubator, the plates were carefully shaken horizontally left and right to evenly distribute the cell colonies in the wells.

3.1.4 Thawing and freezing iPSCs

For thawing one vial of cryopreserved iPSCs, E8 complete medium was warmed to RT and supplemented with ROCK inhibitor (Y 27632, Tocris Bioscience, cat#1254) to a final concentration of 10µM. The frozen vial of iPSCs was partially thawed in a 37^{O}C water bath until a small piece of ice remained, before adding 1 ml of the prepared medium dropwise. 6 ml of the medium was added into one Geltrex-coated well in a 6-well plate, and the thawed cell suspension was transferred to the well while stirring carefully with the 5 ml pipette tip. The plate was placed in the incubator, and the medium was changed into E8 complete medium without ROCK inhibitor after 18 hours and for subsequent feedings of the iPSCs.

Freezing of the stem cells was performed by combining E8 completed medium with 10% (v/v) DMSO and 10µM ROCK inhibitor, then adding 1 ml of the medium per well after incubation with EDTA following the same steps as described earlier for splitting the cells. Each well of cell suspension was transferred to a cryovial and placed in a CoolCell freezing container which allows to lower the temperature by 1^{O}C per minute. The cells were stored in -80^{O}C for one day, then transferred to liquid nitrogen the next day. All the materials used in culturing of iPSCs is listed in Table 1 below.

Table 1: List of materials used in iPSC culturing.

Supplier:	Full name:	Catalogue number:	Size/Volume:	Storage conditions:
Gibco™	Essential E8™ Basal Medium	A15169-01	500 ml	2-8 ^{O}C, protect from light.
Gibco™	Essential E8™ Supplement	A15171-01	10 ml	-5 to -20 ^{O}C, protect from light.
Gibco™	DPBS, no calcium, no magnesium (1x)	14190250	10 x 500 ml	15-30 ^{O}C

Invitrogen™	UltraPure™ 0.5M EDTA, pH 8.0	15575020	4 x 100 ml	RT
Gibco™	Geltrex™ LDEV-Free Reduced Growth Factor Basement Membrane Matrix	A1413201	1 ml	-20 to -80 ^{O}C
Gibco™	Advanced DMEM/F-12	12634010	500 ml	2-8 ^{O}C, Protect from light
Tocris Bioscience	Y-27632 dihydrochloride (ROCK inhibitor)	1254	10 mg	Desiccate at RT

3.1.5 Differentiation process of microglial cells

For the differentiation process of microglia from iPSCs, we applied the protocol based on the previously published paper (46). First in the process the iPSCs are induced into KDR^{+} CD235a^{+} primitive hemangioblast by BMP4 signalling. Then the cells are pushed into the myeloid lineage by supplementation of bFGF, SCF, and VEGFA, and further guided into becoming microglia progenitor cells via inducing them with SCF, IL-3, TPO, M-CSF, and FLT3. A last set of growth factors, M-CSF, FLT3, and GM-CSF are used to further differentiate CD45^{+} CX3CR1^{-} microglial progenitors, into CD14^{+} CX3CR1^{+} microglial progenitor cells. Stimulating these progenitor cells with IL-34 and GM-CSF results in microglial cells and marks the end of the differentiation process (46).

The timeline of the differentiation process is presented in Figure 6.

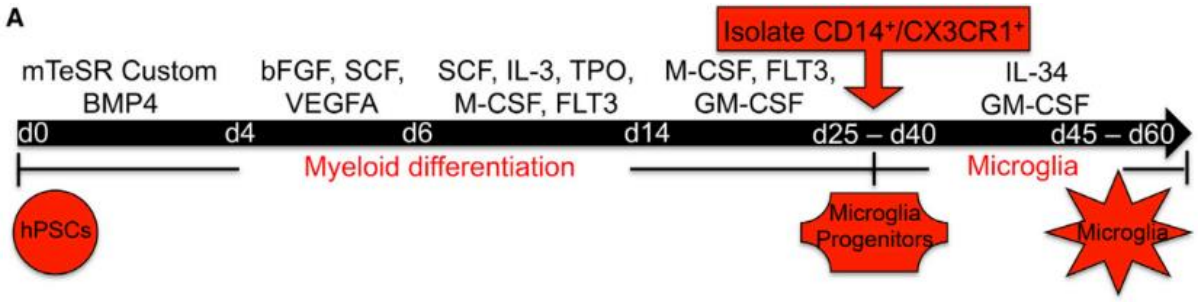

Figure 6: *Timeline of differentiation process from iPSCs into Microglia. (51)*

3.1.6 Differentiation of myeloid progenitors

When the iPSCs reached ~60% confluency, the cells were detached with 0.5mM EDTA and then plated onto a Geltrex coated 6-well plate in mTeSR medium containing 80 ng/ml BMP4,

to induce differentiation into the myeloid lineage. The medium was changed daily for the next 4 days, and then replaced with StemPro-34 SFM supplemented with 25 ng/ml bFGF, 100 ng/ml SCF and 80 ng/ml VEGF. On day 6, the medium was replaced to StemPro-34 containing 50 ng/ml SCF, 50 ng/ml IL-3, 5 ng/ml TPO, 50 ng/ml M-CSF and 50 ng/ml Flt3 ligand. On day 10, the supernatant fraction of cells was pelleted at 600x g for 5 minutes and then resuspended in fresh StemPro-34 medium containing the same concentrations of cytokines. On day 14, the supernatant cells were pelleted at 600x g for 5 minutes again and resuspended in StemPro-34 containing 50 ng/ml M-CSF, 50 ng/ml Flt3 ligand and 25 ng/ml GM-CSF. The culture medium was replaced for the next ten days every other day. After day 24, the cells differentiated into microglia progenitor cells. More details on differentiation media are listed in Table 2.

3.1.7 Differentiation of microglial cells

The myeloid progenitor cells expression was then investigated using flow cytometry. When we observed that a decent amount of our cells was $CD14^+$ $CX3CR1^+$ we continued the differentiation process. The microglia progenitor cells were plated onto tissue-treated dishes in RPMI-1640 supplemented with 2mM GlutaMAX-I, 10 ng/ml GM-CSF and 100 ng/ml IL-34 and the medium was then replenished every three to four days for two weeks. More details on differentiation growth factors are listed in Table 3.

Table 2: Overview of the different mediums used in the differentiation of iPSCs to Microglia.

Supplier:	Full name:	Catalogue number:	Size/Volume:	Storage conditions:
STEMCELL Technologies	mTeSR Complete medium kit	85850	500 ml kit	2-8 °C
STEMCELL Technologies	mTeSR Basal medium	85851	400 ml	2-8 °C
STEMCELL Technologies	mTeSR 5x Supplement	85852	100 ml	-20 °C
Thermo Fischer Scientific	StemPro-34 SFM kit	10639-011	500 ml kit	2-8 °C, Protect from light
Thermo Fischer Scientific	StemPro-34 SFM (1x) medium	10640-019	500 ml	2-8 °C, Protect from light
Thermo Fischer Scientific	StemPro-34 Nutrient Supplement (40x)	10641-025	13 ml	-20 to -5 °C, Protect from light
Gibco™	RPMI-1640 Medium	61870010	500 ml	2-8 °C, Protect from light

W/Glutamax-I (1x)

Table 3: Overview of different growth factors used in the differentiation process.

Supplier:	Full name:	Catalogue number:	Size/Volume:	Storage conditions:
STEMCELL Technologies	Human Recombinant BMP-4	78211	20 µg	-20 to -80 °C
Thermo Fischer Scientific	Gibco™ Human FGF-basic (FGF-2/bFGF) (aa 10-155) Recombinant Protein	PHG0024	10 µg	-20 °C
Thermo Fischer Scientific	Human SCF Recombinant Protein	RP-8631	10 µg	-20 °C
Thermo Fischer Scientific	Gibco™ Human VEGF-165 Recombinant Protein	PHC9394	10 µg	-20 °C
Thermo Fischer Scientific	Gibco™ Human IL-3 Recombinant Protein	PHC0034	10 µg	-20 °C
Thermo Fischer Scientific	Gibco™ Human TPO (Thrombopoietin) Recombinant Protein	PHC9514	10 µg	-20 °C
Thermo Fischer Scientific	Gibco™ Human Flt-3 Ligand (FLT3L) Recombinant Protein	PHC9414	10 µg	-20 °C
Thermo Fischer Scientific	Gibco™ Human GM-CSF Recombinant Protein	PHC2015	10 µg	-20 °C
Thermo Fischer Scientific	Invitrogen™ Human IL-34 Carrier-Free	50-112-3511	10 µg	-20 °C
Thermo Fischer Scientific	Macrophage CSF (M-CSF)	PHC9504	10 µg	-20 °C

3.1.8 Freezing and thawing of myeloid progenitor cells

After checking the expression of our myeloid progenitor cells but before continuation of differentiation into microglial cells, a part of the cells was collected for cryo-preservation. The cells were frozen in cryotubes using freezing medium consisting of 90% Foetal bovine serum (FBS) and 10% (v/v) DMSO. The cells were then transferred to a CoolCell freezing container and placed overnight at -80°C and the next day the cells were transferred to liquid nitrogen for long-term storage.

The thawing process is initiated by transferring the cryotube to a 37°C water bath for 1-2 minutes, until they were partially thawed. The cells were transferred into a 15 ml tube, and RPMI-1640 was added to 5x the original volume of the cryotube, then the cells were centrifuged at 300 g for 6 min, resuspended in 3 ml of RPMI-1640 and plated into culture wells. All materials used in this cryopreservation and thawing process are listed in Table 4 below.

Table 4: Materials used in cryopreservation and thawing of myeloid progenitor cells.

Supplier:	Full name:	Catalogue number:	Size/Volume:	Storage conditions:
Gibco™	HI FBS	16140071	500 ml	-10°C
Gibco™	RPMI-1640 Medium W/Glutamax-I (1x)	61870010	500 ml	2-8 °C, Protect from light

3.1.9 Immunofluorescent stain of IBA1 in differentiated microglial cells

After the end of the microglia differentiation, we wanted to confirm that the cells we had cultured were microglia and so we performed an immunofluorescent (IF) stain using a common microglia marker, IBA1 (Abcam, cat#ab178846). The cells were first fixed with 4% (v/v) paraformaldehyde (PFA, Thermo Scientific, cat#28908) in 1X Phosphate-buffered saline (PBS) for 30 minutes at RT, then washed twice with PBS. Then the cells were blocked with blocking buffer containing 1× PBS, 10% (*v*/*v*) goat serum (Sigma-Aldrich, cat#G9023) with 0.3% (*v*/*v*) Triton™ X-100 (Sigma-Aldrich, cat#X100-100ML) (9036-19-5) for 2 hours at RT. The primary antibody Rabbit Anti-IBA1 (Abcam, cat#ab178846, 1:100) was added to the cells in sufficient volume to completely cover the sample and incubated overnight at 4°C. The next day, the cells were washed with PBS for 2 hours by frequent rinsing, before incubating with Alexa Flour® goat Anti-rabbit 488 (Thermo Fisher Scientific, cat# A11008,

1:800) and Hoechst nuclear counterstain (Thermo Fisher Scientific, cat#62249) overnight at 4°C. Imaging was performed using the Leica DMIL LED (Leica Microsystems) and images captured using the Leica DFC3000 G (Leica Microsystems) camera attachment. Details of all the materials and antibodies used in the IF stain of the differentiated microglial cells are shown in Table 5 below:

Table 5: Overview of materials and antibodies used in IF staining of differentiated microglial cells.

Supplier:	Full name:	Catalogue number:	Size/Volume:	Storage conditions:
Fluidigm Corp	Maxpar PBS	NC1439049	500 ml	15-30 °C
Sigma Aldrich	Goat serum	G9023	10 ml	2-8 °C
Sigma Aldrich	Triton™ X-100	9036-19-5	100 ml	…
Abcam	Recombinant Anti-Iba1 antibody	Ab178846	100 µl	4 °C
Thermo Fisher Scientific	Goat anti-Rabbit IgG (H+L) Cross-Adsorbed Secondary Antibody, Alexa Fluor™ 488	A11008	1 mg	4 °C, Store in dark
Thermo Fisher Scientific	Hoechst 33342 Solution (20 mM)	62249	5 ml	4 °C, Store in dark

3.1.10 Microglia cell line

A commercial microglia cell line HMC3 (ATCC CRL-3304) was used for the positive control of microglial differentiation and lineage. The cells were cultured in Minimum Essential Medium Eagle (EMEM, Sigma Aldrich, cat# M4526) supplemented with 11% FBS in a tissue culture flask. The cell culture was incubated at 37°C, 5% CO_2 and the medium were changed every two to three days. The cells were split with a ratio of 1:3 using TrypLE™ as its gentler on the cells than a Trypsin-EDTA solution. The materials used are listed in Table 6 below.

Table 6: Materials used in culturing of the microglia cell line.

Supplier:	Full name:	Catalogue number:	Volume:	Storage conditions:
Sigma Aldrich	Minimum Essential Medium Eagle (EMEM)	M4526	500 ml	2-8 °C
Gibco	HI FBS	16140071	500 ml	-10 °C
Gibco	TrypLE™	12604013	100 ml	RT

3.1.11 Flow cytometry

To characterize the microglial progenitors, we examined cells for dual expression of CD14 and CX3CR1 using flow cytometry. Both the adherent and floating cells were collected and tested for their dual expression of these two markers. The floating cells were transferred into 15 ml tubes. The adherent cells were washed with 4ml DPBS -/- (ThermoFisher, cat#14190250), then 1 ml TrypLE™ was added to the wells and they were incubated for 5 minutes. After this, we neutralised the TrypLE™ with 2 ml of neutralisation medium and washed the cells with 10 ml of flow buffer (0.5% BSA in PBS). After washing, the cell suspension was transferred to a 50 ml tube for centrifugation, and the two tubes containing our cell fraction were centrifuged at 600x g for 5 minutes. We then aspirated the supernatant and resuspended the cell pellet in 100 µl of flow buffer and counted the cells in the countess to determine the antibody dilution to use. The cells were incubated with the CD14 (1:100) and CX3CR1 (1:100) antibodies for 40 minutes at 4 °C in the dark. The cells were then centrifuged at 300x g for 10 minutes, the supernatant was aspirated, and the cells were resuspended in 200 µl flow buffer. The samples were analysed in BD (LSRFortessa™) flow cytometer to determine the peak of CD14/CX3CR1 double positive progenitor cells. Details of the antibodies and materials used in the flow experiments are listed in Table 7 below.

Table 7: Overview of antibodies and materials used in flow experiments.

Supplier:	Full name:	Catalogue number:	Size/Volume:	Storage conditions:
BioRad	CD14-APC	MCA596APC	100 tests	4 °C
R&D Systems	CX3CR1-PE	FAB5204P-025	25 tests	2-8 °C
Gibco™	DPBS, no calcium, no magnesium (1x)	14190250	10 x 500 ml	15-30°C
Gibco™	TrypLE™	12604013	100 ml	RT

3.2 Characterisation of CSF cells

3.2.1 Cytospin

For a part of the project, we wanted to test a tried-and-true method in haematology, Cytospin, a machine that uses centrifugal force to fix blood cells on microscope slides. The conventional protocol however, was not suitable for CSF cell analysis directly and required optimisation. First, we tested the area and density of cells in the area of a microscope slide for the cytospin. Several concentrations of cells (50000-500000/200µl) were tested for optimal dispersal of cells onto the slides. The experimental procedure was as follows, firstly, we

thawed a 1ml sample of $3x10^6$ proteomic stabilized cells, then centrifuged them at 800 rpm for 5 minutes and then resuspended them in required amount of PBS to acquire the volumes we wanted to test. An image of the Cytospin machine and the slide setup for the machine can be seen below in Figure 7. The resuspension volumes can be seen below in Table 8.

Figure 7:*Image of the Cytospin machine and the cytofunnel-slide setup.*

Table 8: Resuspension volumes to acquire desired cell volumes for Cytospin tests.

Number of cells (In Thousands)	Volume of cell suspension	Volume of PBS added	Total Volume
50	16.6 µl	183.4 µl	200 µl
100	33.3 µl	166.7 µl	200 µl
200	66.6 µl	133.4 µl	200 µl
300	100 µl	100 µl	200 µl
400	133.3 µl	66.7 µl	200 µl
500	166.6 µl	33.4 µl	200 µl

The clinical cytospin at the haematology department was used in the experiment and each sample was loaded and the Cytospin centrifuged at 400 rpm for 4 minutes. Images of the cells on the microscope slides, were taken with the Zeiss LSM 900 (Zeiss microscopy) and are presented in results. Lastly, all the materials used in the Cytospin experiment are listed in Table 9.

Table 9: Materials used in Cytospin experiments.

Supplier:	Full name:	Catalogue number:	Size/volume:	Storage conditions:
Maxpar Corp	Maxpar PBS	NC1439049	500 ml	15-30 ^{O}C
Thermo Scientific	Epredia X50 Microscope slide	15998086	50 slides	RT

Sarstedt	Screw cap tube, 15 ml	62.554.502	15 ml	Sterile, RT

3.2.2 Fixation

After the Cytospin test we decided to investigate methods of fixation of the cells to the microscope slides with the aim of preserving epitopes. One method that we found to be promising was air-drying cells on slides before fixing them to the slide itself. To solve our limitations with the actual CSF samples, which was the very low cell count, and keeping cell density appropriate and obtaining a small, contained area of cells on the slide itself for time and cost-effective Hyperion analysis, we used a cell gasket (Sigma Aldrich, cat# GBL103250-10EA) designed to give small wells with an area of 7 mm^2 per well in our tests. For all our tests we used buffy coated cells, firstly thawing a 1ml sample of these containing $3x10^6$ cells, then we aspirated 100 µl from the main sample into an eppendorf tube and added 20 µl Thaw-lyse buffer before centrifuging this at 800g for 7 minutes. Then we aspirated the supernatant and resuspended the cell pellet in 50 µl distilled water, moved to a laminar flow hood, and attached the cell gasket to the microscope slide, then loaded our samples in 4 different wells in the centre of the slide. After loading we let the samples air-dry on the slide inside the hood for 30 minutes, before removing the cell gasket from the slide and dipping the slide in a coplin jar which contained 4% PFA for 10 minutes. Then we rinsed the residual PFA from the slide by dipping it in first a coplin jar containing PBS for 10 minutes and then in distilled water for 10 minutes. We performed multiple tests of this method to optimize multiple aspects of the process which will be shown in results. An image of the cell gasket is shown below in Figure 8. Finally, all the materials used in the fixation experiments are shown in Table 10 below.

Figure 8: *Image of the cell gasket used in fixation experiments.*

Table 10: Overview of materials used in fixation experiments.

Supplier:	Full name:	Catalogue number:	Size/Volume:	Storage conditions:
Thermo Scientific	Epredia X50 Microscope slide	15998086	50 slides	RT
Sigma Aldrich	Grace Bio-labs reusable CultureWell™ gaskets	GBL103250-10EA	10 gaskets	RT
Smart Tube	THAWLYSE1 "Thaw-Lyse buffer, 1000X concentrate"	180717A	60 ml	RT
Maxpar Corp	Maxpar PBS	NC1439049	500 ml	15-30 ^{O}C
Thermo Scientific	Pierce™ 16% Formaldehyde (w/v), Methanol-free	28908	10 x 10 ml	RT

3.2.3 IMC Staining

After optimising the method to fix CSF cells onto a slide, the cells were stained for mass cytometry imaging (Hyperion). The cell gasket from the fixation tests and protocol, allowed the use of small wells with different samples on the slide that were ready for staining. The experimental set-up for our slide was as follows, using only the most centre wells of our slide, we had one well containing CSF samples, one well containing our differentiated microglial cells, one well containing the CRL-3304 Microglia cell line, one well containing peripheral blood mononuclear cells (PBMCs), and one well containing buffy-coated blood

cells. In addition, we had 2 replicates of each well on the plate as well, so that we had 3 replicates in total. With CRL-3304 being our positive control in this experiment, and the buffy-coated blood cells being our negative control. Each of our wells had an area of 7mm^2, and with 15 wells in total, the total area of our experimental set-up was 105 mm^2. An illustration of our experiment setup is shown in Figure 9 below.

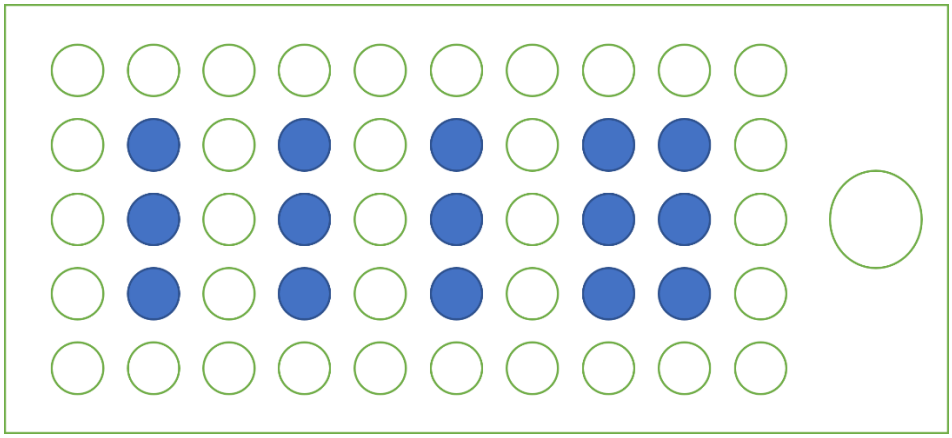

Figure 9: *Illustration of experimental setup for Hyperion staining experiments. Blue circles are used wells, and white circles are empty. Going from left to right, the different columns contained the following samples: CSF, iPSCs-derived microglia, CRL-3304 microglia cell line, PBMCs, and buffy coats.*

Before starting we prepared the antibody cocktail and kept it on ice. Then, we circled the area of the wells for each sample type using a PAP pen. The PAP pen is extremely hydrophobic, so using it to create a barrier around the sample types allows us to apply blocking solution or antibody solution directly onto the slide. Special car was taken when pipetting any solution onto the slides as it is possible to wash away fixated cells. With the barrier in place around the samples we added 550 µl FC-receptor blocker to each sample area, and incubated for 10 minutes at RT, aspirated the FC blocker of the slide then added the antibody cocktail and incubated at 4 °C overnight. The next day the slide was washed in CSB for 10 minutes by dipping the slide into a coplin jar, after this a second wash in Maxpar H_2O for 15 minutes in a coplin jar was performed. After the washes were complete, we stained our samples with 550µl, 500µM, Intercalator-Ir (IR) in Fix and Perm buffer for 1 hour at RT. Afterwards we aspirated the IR solution of the slide and then washed it in Maxpar H_2O for 10 minutes in a coplin jar. The final step was then to Air-dry the slide in a laminar flow hood for at least 20 minutes at RT. When the slide was completely dry, we checked our samples in a microscope before storing it in a slide box and taking it to the Hyperion. All materials used in the staining of our samples are listed in Table 11 below, and the antibody panel used in preliminary experiments along with dilutions are listed in Table 12 below. The antibody panel used in final experiments along with dilutions are listed in Table 13 below.

Table 11: list of all materials used in IMC staining protocol

Supplier:	Full name:	Catalogue number:	Volume:	Concentration:	Storage conditions:
Miltenyi Biotec	FcR Blocking Reagent, Human	130-059-901	2 ml	-	Protect from light. 2-8 °C
Fluidigm®	Maxpar® Cell Staining Buffer	201068	500 ml	-	2-8 °C
Standard Biotools	Cell-ID™ Intercalator-Ir	201192B	500 µl	500 µM	-20 °C
Thermo Scientific	Pierce™ 16% Formaldehyde (w/v), Methanol-free	28908	10 x 10 ml	-	RT
Fluidigm®	Maxpar® Water	201069	500 ml	-	4 °C
Fluidigm®	Maxpar® Fix and Perm Buffer	201067	100 ml	-	2-8 °C

Table 12: Antibody panel used in preliminary tests of Hyperion staining protocol

Metal	Tag	Antibody	Clone	BB – Dilution	Backbone Ab (500 ml)
89	Y	CD45	HI30	400	1.25
141	Pr	CD49d/α4 integrin	9F10	200	2.5
142	Nd	CD73	606112	200	2.5
143	Nd	HLA-DR	L243	1600	0.3125
144	Nd	CD146	P1H12	200	2.5
145	Nd	CD117	104D2	200	2.5
146	Nd	CD8a	RPA-T8	200	2.5
147	Sm	CD20	2H7	400	1.25
148	Nd	CD34	581	200	2.5
149	Sm	CD25 (IL-2R)	β	100	5
150	Nd	CD105	166707	200	2.5
151	Eu	CD278/ICOS	C398.4A	200	2.5
152	Sm	CD66b	80H3	400	1.25
153	Eu	CD194 (CCR4)	205410	400	1.25
154	Sm	CD49f	MP4F10	400	1.25
155	Gd	CD161	HP-3G10	200	2.5
156	Gd	CD184 (CXCR4)	12G5	200	2.5
158	Gd	CD27	L128	200	2.5
159	Tb	CD45RO	UCHL1	400	1.25

160	Gd	CD44	BJ18	1600	0.3125
161	Dy	CD235b	HIR2	400	1.25
162	Dy	CD11c	Bu15	400	1.25
163	Dy	CD33	WM53	200	2.5
164	Dy	CD133		200	2.5
165	Ho	CD127 (IL7-Ra)	A019D5	200	2.5
166	Er	CD123 (IL-3R)	A019D5	200	2.5
167	Er	CD162	KPL-1	200	2.5
168	Er	CD185 (CXCR5)	51505	200	2.5
169	Tm	CD90	5E1	200	2.5
170	Er	CD45RA	HI100	800	0.625
171	Yb	CD195 (CCR5)	NP-6G4	200	2.5
172	Yb	CD38	HIT2	200	2.5
173	Yb	CD196/CCR6	G034E3	200	2.5
174	Yb	CD135	EH12.2H7	200	2.5
175	Lu	CD10	HIR2	400	1.25
176	Yb	CD56		400	1.25
209	Bi	CD16	VI-PL2	200	2.5
112	Cd	CD4	RPA-T4	1600	0.3125
113	Cd	CD14	M5E2	100	5
114	Cd	CD19	HIB19	100	5
116	Cd	CD3	UCHT1	1600	0.3125
Antibody in total:					73.75
Buffer to add:					426.25

Table 13: Antibody panel used in Hyperion staining

Metal:	**Tag:**	**Antibody:**	**Clone:**	**BB-dilution:**	**Backbone Ab (800 µl)**
89	Y	CD45	HI30	400	2 µl
141	Pr	CD235b	HIR2	400	2 µl
142	Nd	CD19	HIB19	400	2 µl
143	Nd	HLA-DR	L243	1600	0.5 µl
145	Nd	CD4	RPA-T4	200	4 µl
146	Nd	CD8a	RPA-T8	200	4 µl
147	Sm	CD20	2H7	400	2 µl
148	Nd	CD34	581	200	4 µl
152	Sm	CD66b	80H3	400	2 µl
153	Eu	TMEM119	-	200	4 µl
154	Sm	CD3	UCHT1	1600	0.5 µl
160	Gd	CD14	M5E2	200	4 µl
162	Dy	CD11c	Bu15	400	2 µl
163	Dy	CD33	WM53	200	4 µl
209	Bi	CD16	VI-PL2	200	4 µl
Antibody in total:					41 µl

Cell Staining Buffer to add:	759 µl

4. Results

4.1 Differentiation of iPSCs into microglia

4.1.1 Differentiation of myeloid progenitor cells from iPSCs

Throughout the differentiation process of the iPSCs into microglia, we observed the cells in the microscope and took images regularly to observe their morphology and the changes thereof. In all the images captured one common trend is observed, a very high confluency. Two days after the differentiation was induced through culturing in medium supplemented with 80 ng/ml BMP4 the first image was taken. This is very early on in the differentiation process and at this stage, cells exhibit normal iPSC morphology and few differentiated cells, a hallmark of early differentiation. Images were captured routinely with an interval of approximately 4 days. An image detailing different stages of the differentiation into myeloid progenitor cells is shown in Figure 10 below.

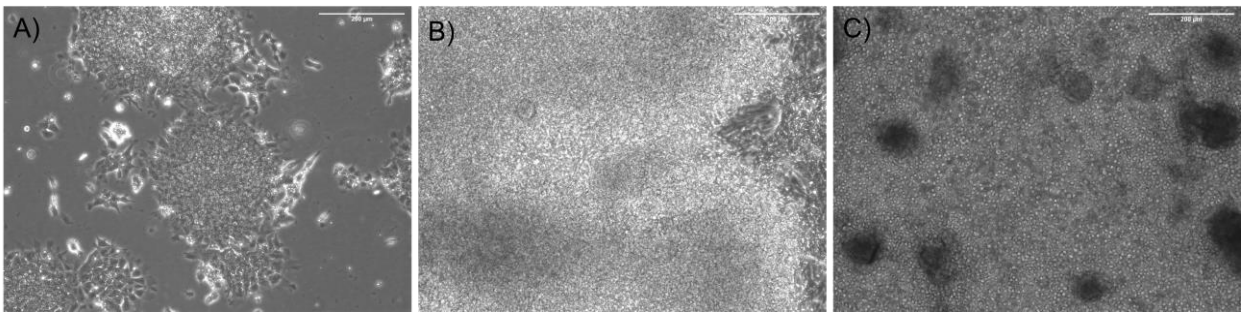

Figure 10: *Images of the control cell line 1, A) 2 days after induction of differentiation, B) 8 days after induction of differentiation, C) 25 days after induction of differentiation, all taken at 10x magnification. Scale bar is 200 µm.*

The iPSCs shown in Figure 10 A) are at this stage exhibiting normal iPSC morphology and few differentiated cells, a hallmark of early differentiation. While Figure 10 B) and C) are respectively showing high and extremely high confluency. Both have lost some of the characteristics of normal iPSC morphology and in B) There are more differentiated cells on the edges of the colony in view, while in C) there are many cells growing on top of each other. All images in Figure 10 are from the same control cell line and from the same cell well.

To facilitate further work with the myeloid progenitor cells we tested whether these could survive cryo-preservation and showed that cells could in fact be successfully expanded and differentiated with minimal loss after cryopreservation. After thawing the cells and 1 day of

incubation, we counted the adherent progenitor cells and observed an average of over 90% viability. The cell count results are shown in Figure 11 below.

Figure 11: *Cell count results of adherent myeloid progenitor cells.*

4.1.2 Characterisation of the myeloid progenitors derived from iPSCs

$CD14^+$ $CX3CR1^+$ are markers used for identification of myeloid progenitors during the differentiation process at day 35 (Figure 6) into microglia progenitor cells. To assess the percentage of $CD14^+$ $CX3CR1^+$ double positive cells we used flow cytometry. The results allowed us to determine if the concentration of these double positive cells in our culture was suitable for further differentiation toward microglia. The expression of double positive progenitors in both the supernatant and adherent cell populations are shown in Figure 12 & 13 below.

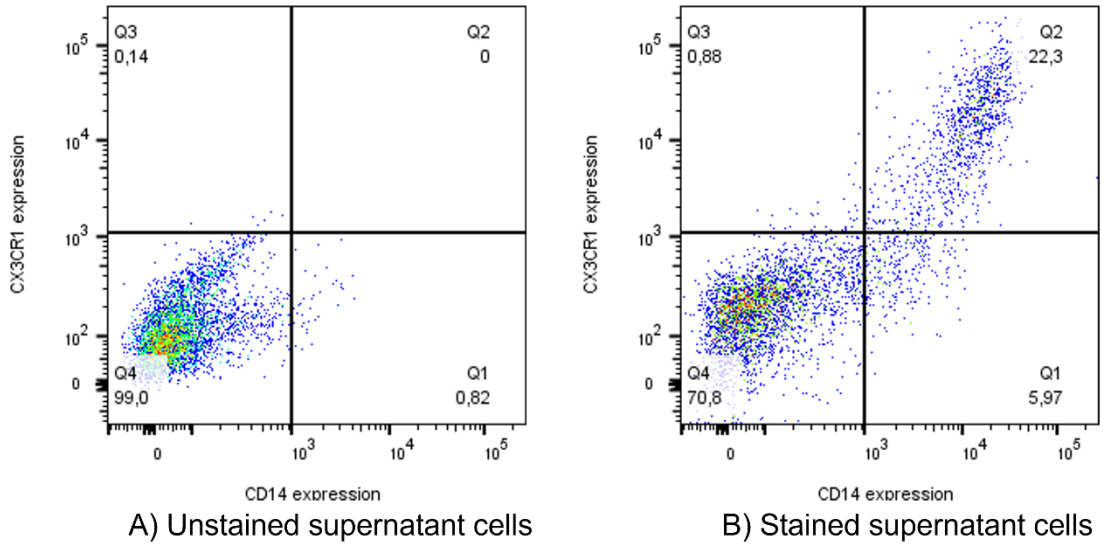

Figure 12: *Flow cytometry showing CD14+ CX3CR1+ cells in A) unstained supernatant cells, and B) stained Supernatant cells. X axis shows CD14 expression, Y axis shows CX3CR1 expression.*

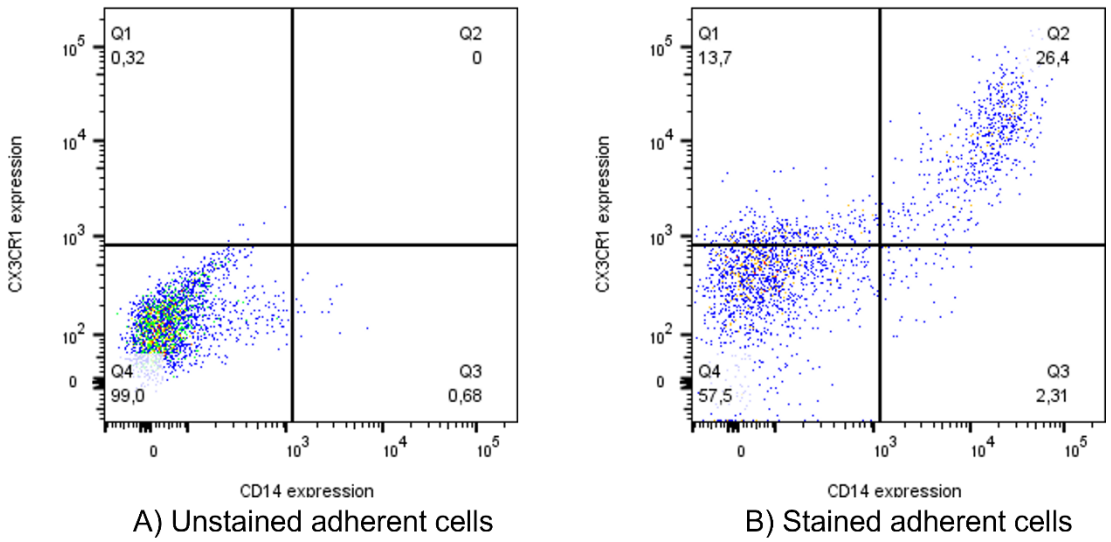

Figure 13: *Flow cytometry showing expression of CD14+ CX3CR1+ cells in A) unstained adherent cells, and B) stained adherent cells. X axis shows CD14 expression, Y axis shows CX3CR1 expression.*

4.1.3 Differentiation from myeloid progenitors into microglial cells

About 25-30% of adherent and suspended cells in the cultures showed double staining for $CD14^{+}$ $CX3CR1^{+}$. This concentration of microglial progenitor cells was in the expected range and suitable for further differentiation steps into microglia. We initiated the final stages of differentiation using medium induced with 100 ng/ml IL-34 and 10 ng/ml GM-CSF. As shown in Figure 14, the cells changed from their globular shape to a more elongated shape, reflecting the differentiation process as expected. The image in Figure 14 is of the same control line, and from the same cell culture well as Figure 10, in the differentiation process at 42 days after the start of differentiation and 1 week after induction with 100 ng/ml IL-34 and 10 ng/ml GM-CSF. The cells in the image are microglial progenitor cells. Figure 14 is shown below.

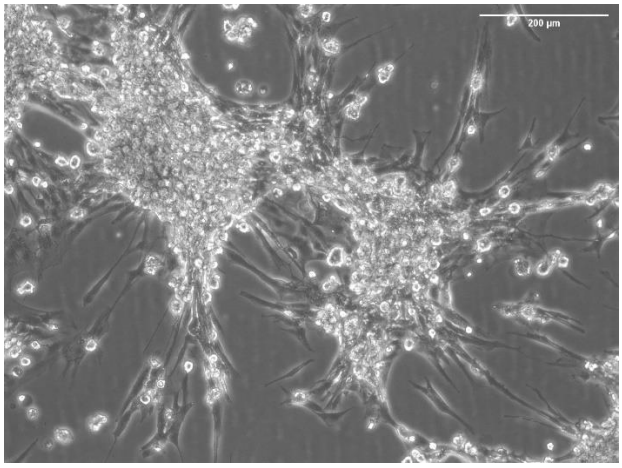

Figure 14: *Picture of the control cell line 1, 42 days after induction of differentiation, taken at 10x magnification. Scale bar is 200 µm.*

At the final stage of the differentiation, we confirmed that the cells were microglia by IF stain using a common microglia marker, IBA1 and a nuclear staining marker (Hoechst 33342 Solution). The results of the IF stain are shown in Figure 15 below.

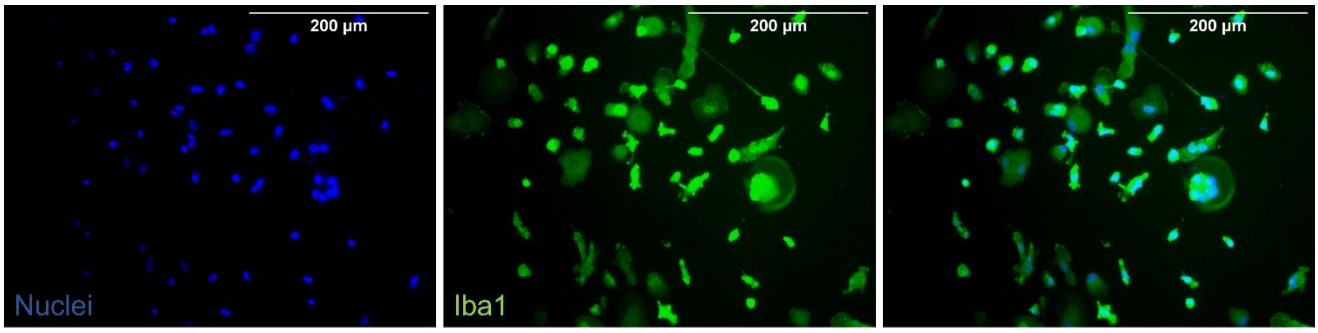

Figure 15: *IF stain of fully differentiated cells, two single channels of nuclei (blue) and IBA1 (green) and a composite image of the stain. All pictures are taken on 20x magnification. Scale bar is 200 µm.*

In Figure 15 the cells show distinct modified morphology compared to earlier in the differentiation process and shown in both Figure 10 & 14. Further the staining clearly shows an abundant expression of IBA1 in our differentiated microglial cells.

4.2 Characterisation of CSF cells

4.2.1 Establishment of an optimized IMC analysis pipeline for single cells from the CSF

The major aim of the project was the development and optimization of a technique to characterise single cells on the Hyperion. This required a method to fixate the cells onto microscope slides, so they could be used with the Hyperion. Of note, the CSF cells are in suspension. The first method we tested was a standard haematology method, the cytospin as described in 3.2.1 Investigating the central area of cell deposition of each cell volume, we compared the concentration of cells between the different cell volumes. The cell volumes we tested were in the range of .05-.5x10^6, and the results of the cytospin test are shown in Figure 16 below.

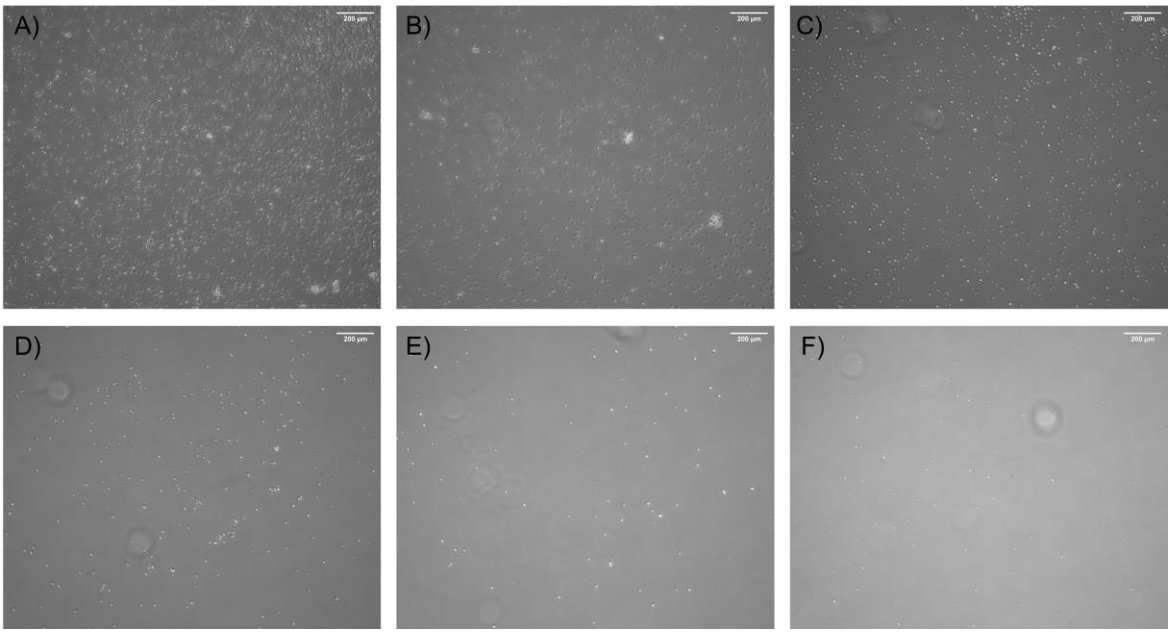

Figure 16: *Results of Cytospin test. Cell numbers are A) 500 000, B) 400 000, C) 300 000, D) 200 000, E) 100 000, F) 50 000. Scale bar is 200 µm.*

The Cytospin test performed well, but we discovered, our CSF cell concentrations were much lower than the lowest in the cytospin test which was 50 000 cells/200 µl (which equals to 250 cells/µl). Figure 16 (F) shows the sparce deposition of the cells when using the cytospin working at the concentration of 250 cells/µl. We conclude that the cytospin was not an optimal setup for the IMC analysis as the cost-effective ablation requires the cells to be in close proximity to each other.

The most promising solution to the cell density problem for IMC was elegantly simple, combining a cell gasket and letting the cells dry onto the slide while inside a laminar flow hood, before then using 4%PFA to properly fixate the cells onto the slide. As this approach was novel, it had certain challenges and required optimization. The suspension medium first used was Maxpar PBS and caused, crystallization in the drying process. Thus, we changed to distilled H_2O which resolved the issue. The results of both are shown in Figure 17 below.

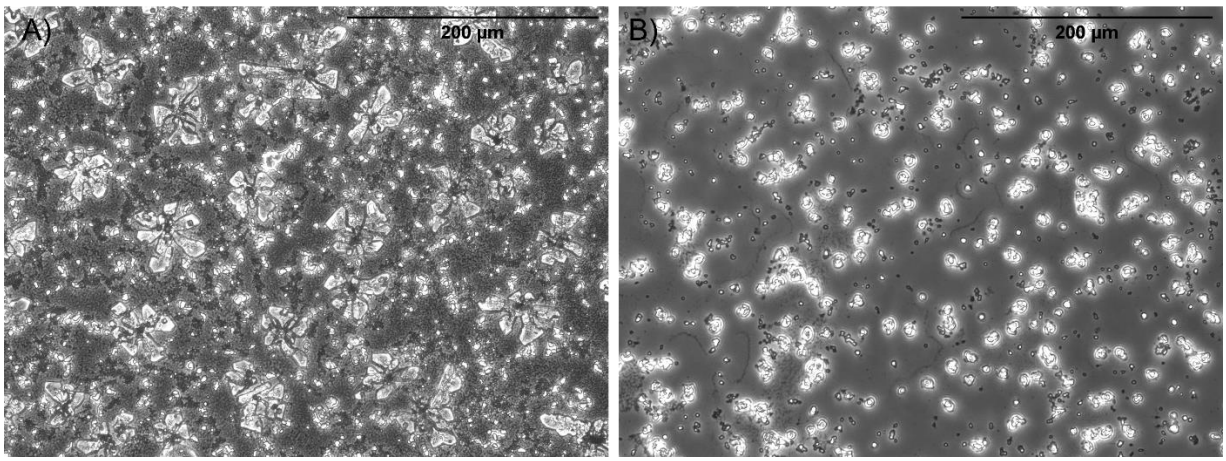

Figure 17: *Pictures of the effect on our cells by resuspension with two different mediums. A) Shows resuspension with PBS. B) Shows resuspension with dH20. Both images are taken on 20x magnification. Scale bar is 200 µm.*

Next, we tested the effect of different fixation times, 5 minutes vs 10 minutes with PFA. It is crucial to optimize the fixation protocol to obtain adequate adherence of cells to the microscope slides while maintaining epitopes for antibody binding.

Next, we tested our antibody staining method for the Hyperion. Buffy coat samples were utilized for the optimization experiments. Firstly, we tried using an incubation time of 30 minutes at RT for the antibody cocktail, an overnight stain of the Intercalator-IR at 4°C, and the immune marker antibody panel that our group had previously developed and optimised. The immune marker antibody panel for this experiment is shown in Table 12. The results of which are shown in Figure 18 down below.

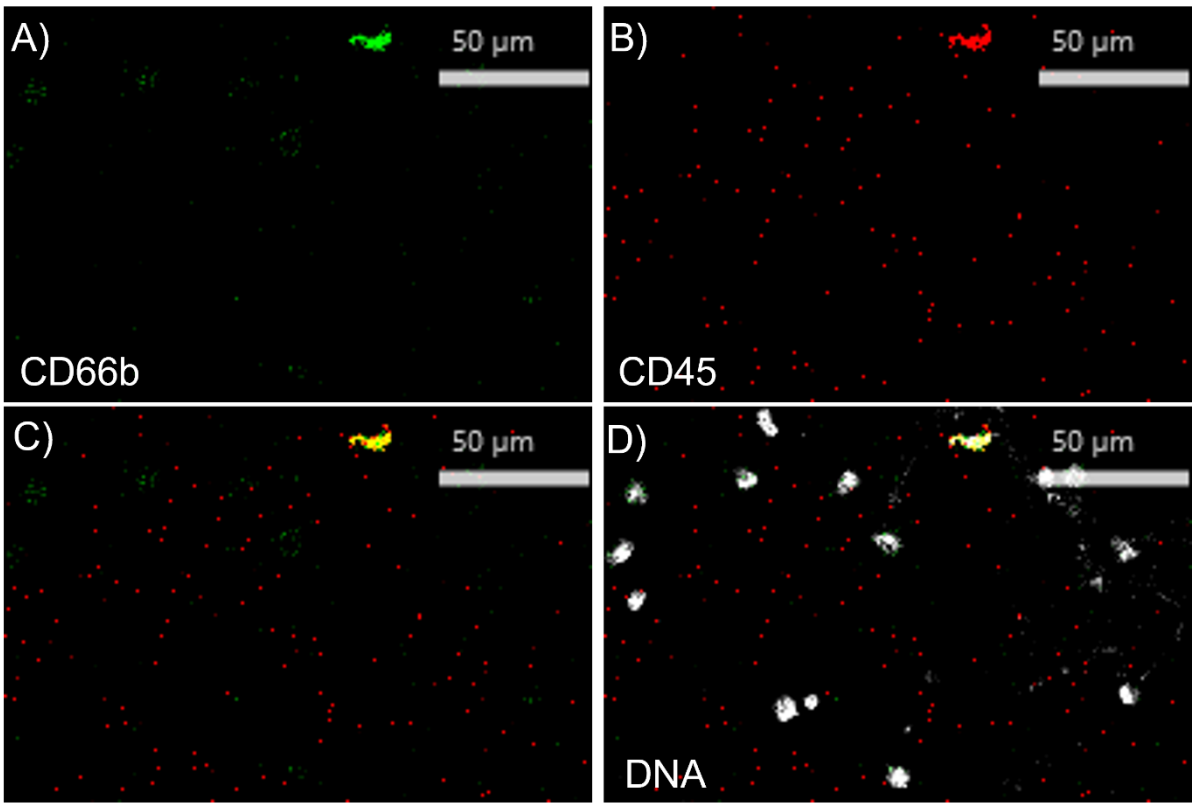

Figure 18: *Results of the first Hyperion experiment of buffy coats. Showing the CD66b staining (Green) (A), the CD45 staining (Red) (B), a composite image of both stains (C) and a composite image of both stains and an intercalator-DNA stain (White) (D). Scale bar is at 50µm.*

As we can see in Figure 18 for buffy coat samples that contain all leukocytes the antibody markers CD66b (A) and CD45 (B) are shown alongside two composites, one without the Intercalator-DNA (C) and one with (D). The channels for any other antibodies on the panel is not shown because of a high amount of background staining and required optimization. Figure 18 (C, D) shows that CD66b and CD45 had little unspecific binding, and specific binding for neutrophils that are $CD66b^+$ and $CD45^+$ positive cells. Buffy coats contain about 80% neutrophils, with the remaining 20% consisting of a mixture of lymphocytes, monocytes, and platelets.

For further optimization based on the results of the, Hyperion experiment we tested an overnight staining of the antibody cocktail at 4°C, reducing the intercalator incubation to 1 hour at RT, while using the antibody panel shown in Table 12. The results of this test are shown in Figure 19 down below.

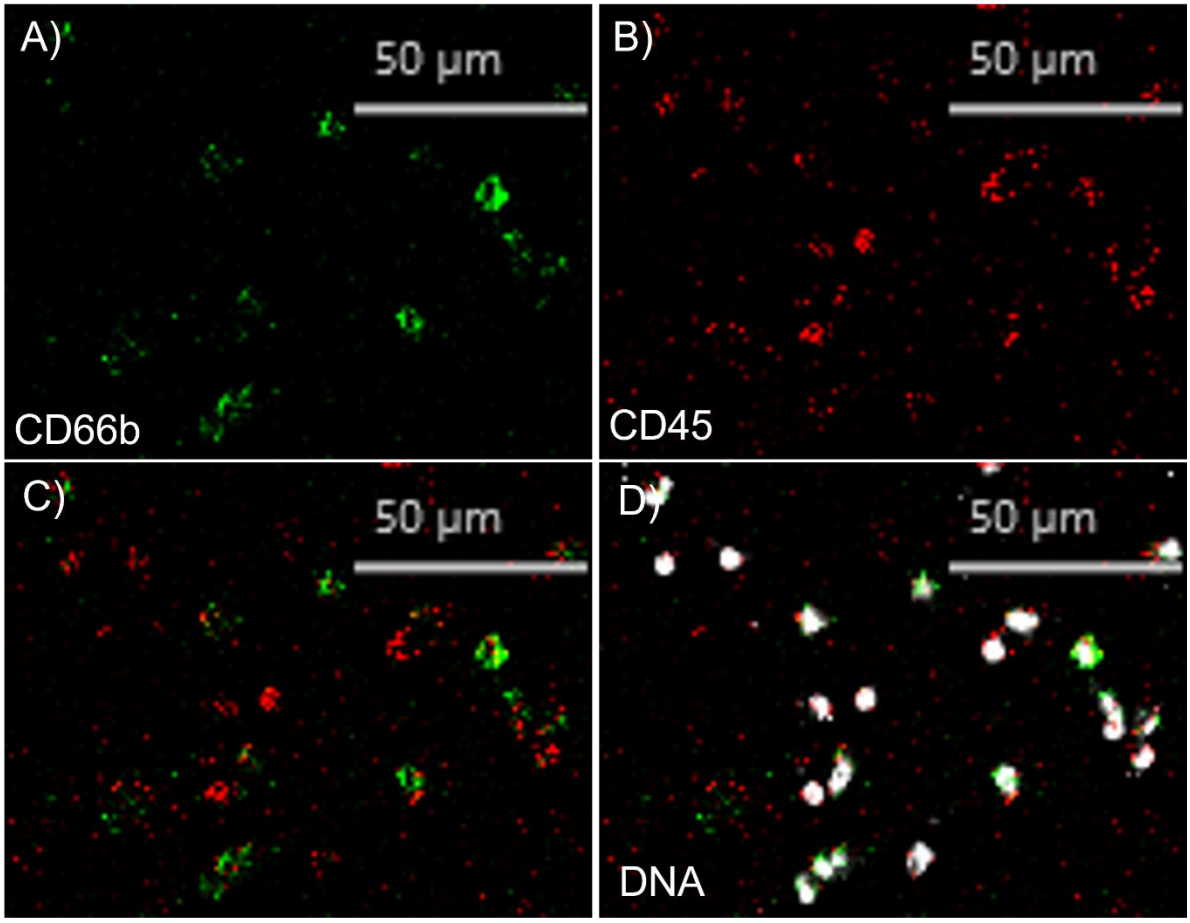

Figure 19: *The results of the second Hyperion staining experiment of buffy coats. Showing the CD66b staining (Green) (A), the CD45 staining (Red) (B), a composite image of both stains (C) and a composite image of both stains and an intercalator-DNA stain (White) (D). Scale bar is 50µm.*

The results in Figure 19 show that the extended antibody incubation substantially increased staining specificity overall. On the other hand, the reduction of incubation time for the Intercalator-DNA did affect the nuclei staining quality. Figure 19 (C, D) shows specific antibody binding of both CD45 and CD66b on multiple cells and reduced background staining.

4.2.2 Immunophenotyping of CSF cells with IMC

Next, we used the optimized Hyperion protocol in our main experiment of CSF cells. The sample types included in the main experiment were: CSF samples, iPSCs-derived microglia cells, the CRL-3304 microglia cell line, PBMCs, and buffy coated cells. The antibody panel used in this experiment is shown in Table 13. Of note, the CSF samples were pooled from different donors, and we observed red blood cells that normally should not be in CSF samples. The high concentration of red blood cells increased the difficulty of finding immune cells to determine areas of ablation in the Hyperion. The results of an ablated area for

Hyperion analysis from one CSF sample of the main Hyperion experiment is shown in Figure 20 below.

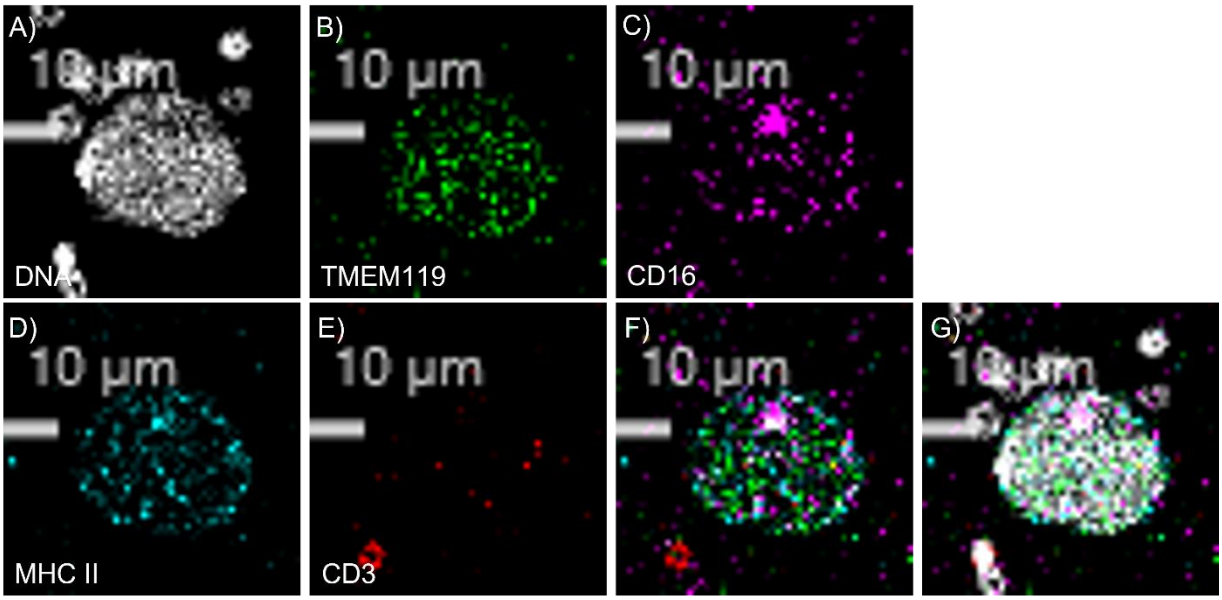

Figure 20: *Hyperion stain of a microglia cell and the adjacent cells in the CSF samples. This staining shows the channel for DNA (White) (A), TMEM119 (Green) (B), CD16 (Purple) (C), MHC II (Cyan) (D), CD3 (Red) (E), and two composites, one without DNA (F) and one with (G). The scale bar is 10µm.*

The microglia images in Fig 20 of a CSF sample, show the staining patterns for DNA (A), TMEM119 (B), CD16 (C), MHC II (D), CD3 (E), and two composites, one without DNA (F) and with DNA (G). Figure 20 shows the single microglia-like cell in the ablated area, which shows expression of $TMEM119^{+}$, $CD16^{+}$, MHC II^{+}, and $CD3^{-}$, this expression is best shown in composite image (F). We also observe in (E), (F), and (G) $CD3^{+}$ expression on a smaller single cell in the lower left corner of the ablated area, a marker for T cells.

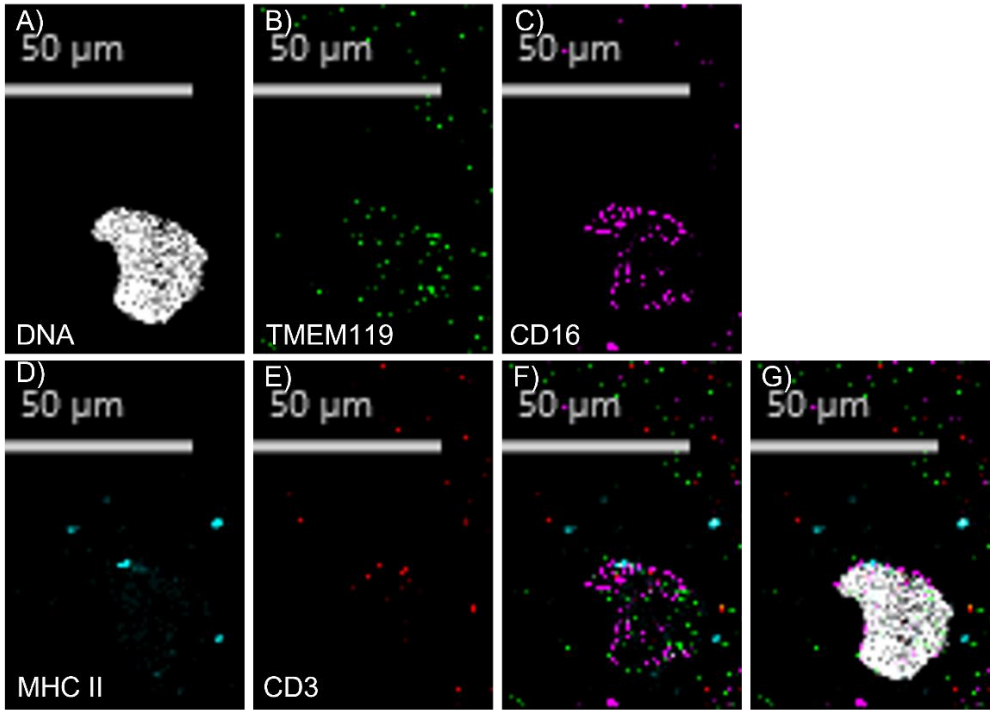

Figure 21: *Hyperion stain of a microglia cell from the sample containing iPSC-differentiated microglia. This staining shows the channels for DNA (White) (A), TMEM119 (Green) (B), CD16 (Purple) (C), MHC II (Cyan) (D), CD3 (Red) (E), and two composites, one without DNA (F) and one with DNA (G). The scale bar is 50µm.*

The images of a differentiated microglia cell is shown in Figure 21. Here, we observe specific expression of $CD16^{+}$, MHC II^{+}, $TMEM119^{+}$ and $CD3^{-}$ on the central cell visible in the stain, this expression is best visualised in the composite image (F).

The results of an area of the CRL-3304 microglia cell line sample from the same experiment is shown in Figure 22 down below.

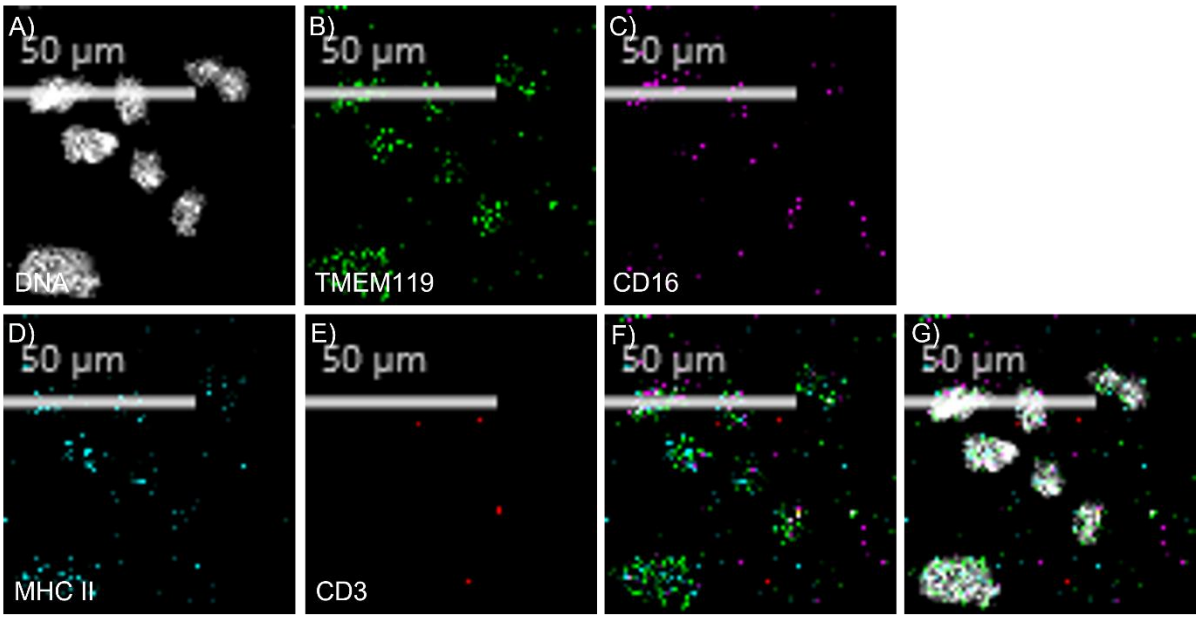

Figure 22: *Hyperion stain of multiple microglial cells from the sample containing the CRL-3304 microglia cell line. This staining shows the channels for DNA (White) (A), TMEM119 (Green) (B), CD16 (Purple) (C), MHC II (Cyan) (D), CD3 (Red) (E), and two composites, one without DNA (F) and one with DNA (G). The scale bar is 50µm.*

Figure 22 shows us the CRL-3304 microglia cell line sample as mentioned. This Figure shows stronger expression of TMEM119^{+}, CD16^{+}, MHC II^{+} and CD3^{-} which is shown clearly in the composite image (F).

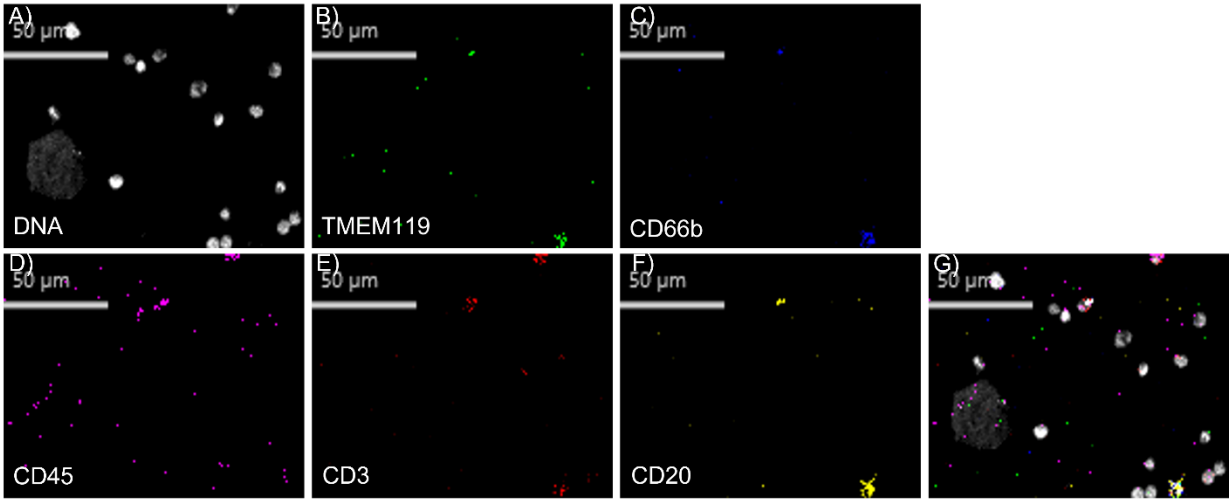

Figure 23: *Hyperion stain of cells from the PBMC sample. This staining shows the channels for DNA (White) (A), TMEM119 (Green) (B), CD66b (Blue) (C), CD45 (Purple) (D), CD3 (Red) (E), CD20 (Yellow) (F), and one composite with the DNA (G). The scale bar is 50µm.*

The staining results of both our controls, PBMC and buffy coat samples, showing specific expression of DNA, TMEM119, CD66b, CD45, CD3, and CD20 from this experiment is presented in Figure 23 and 24. Figure 23 (D, E and G) shows us specific expression of CD3^{+}

on two cells up in the top part of the image, and $CD45^+$ on one of those cells. While Figure 23 (B, C, F and G) shows us specific expression of $TMEM119^-$, $CD66b^-$, and $CD20^-$ on the cells visible in the sample.

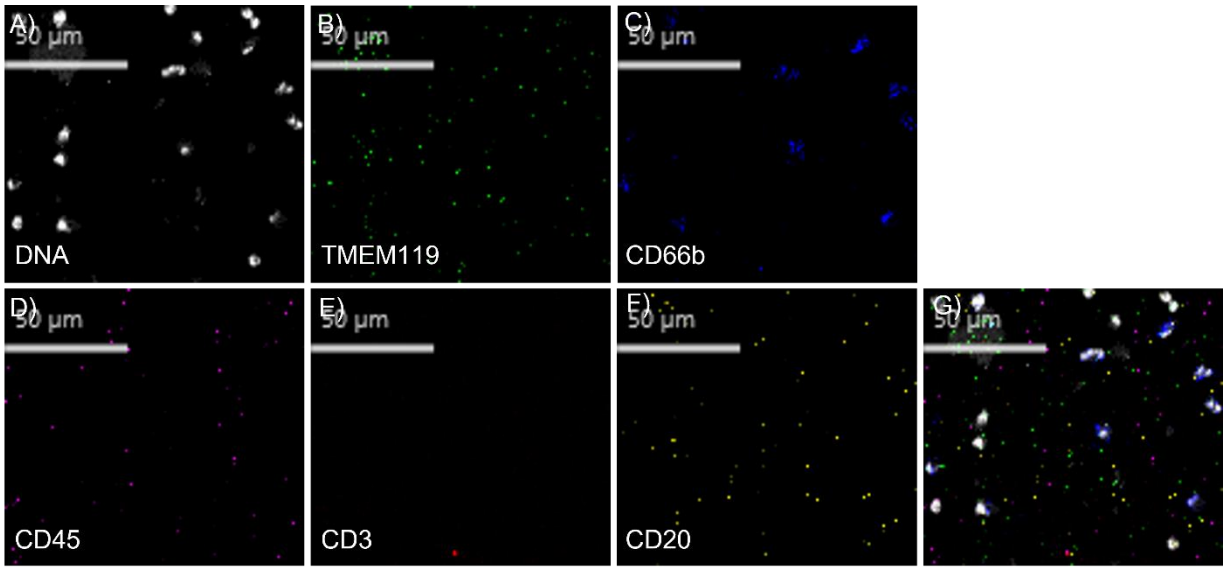

Figure 24: *Hyperion stain of the sample containing Buffy coated cells. This staining shows the channels for DNA (White) (A), TMEM119 (Green) (B), CD66b (Blue) (C), CD45 (Purple) (D), CD3 (Red) (E), CD20 (Yellow) (F), and one composite with the DNA (G). The scale bar is 50µm.*

In the buffy coat samples, Figure 24, we observed neutrophils with specific expression of $CD66b^+$ and $TMEM119^-$, $CD45^-$, $CD3^-$, and $CD20^-$ (B, C, D, E and F). DNA-intercalator staining is specific for the cells, as observed in part (A) of Figure 24. Part (G) is the composite figure of all the different single staining channels together, we observed higher proportion of neutrophils here, as mentioned earlier, with overlapping DNA-intercalator and $CD66b^+$ expression.

5. Discussion

5.1 Differentiation of iPSCs into microglia

The published protocol we used to differentiate microglia from iPSCs worked well with the iPSCs our laboratory induced from fibroblasts of healthy controls. One major concern observed was the consistently high confluency of cells in the wells, as depicted in Figure 10C, where cells appeared clustered. This high confluency potentially could have affected the outcome of the differentiation process since dead cells may affect the remaining cells in the wells. The high confluency was a result of initiating the differentiation stage when the iPSCs had reached approximately 60% confluency and the problems with dead cells could have been avoided by inducing differentiation at an earlier stage, around 30% confluency.

However, induction of differentiation earlier may have led to lower microglia numbers per well. Differentiation of cells from iPSCs is a balance of timing and induction and needs careful planning and execution. In this work, we clearly show microglia marker expression on the derived cells and concluded that the process worked, despite our concerns of high confluency. iPSCs are a great resource for disease specific differentiation of cells such as microglia from MS patients and we expect will be crucial in future personalised in vitro models.

One aspect of long procedures such as the microglia derived from iPSCs is the timing of biobanking of intermediate samples for experiments. In this thesis we succeeded to cryopreserve the progenitor cells before full differentiation to microglia. The results obtained from cryopreservation and subsequent thawing of $CD14^+$ and $CX3CR1^+$ progenitor cells, (Figure 11), were highly promising. The data revealed a total of $3.87x10^5$ cells, with 97% ($3.75x10^5$) being viable and only 3% ($1.17x10^4$) being non-viable. These viability results were notably higher than the original viability reported in the method paper, which stated 57% ± 5% (46). This improvement in viability demonstrates the effectiveness of our cryopreservation technique for preserving the integrity and viability of myeloid progenitor cells. Cryopreservation is crucial for successful biobanking of differentiated progenitor cells for later use since the complete differentiation process is time consuming.

iPSCs derived progenitor cells must express distinct markers of myeloid lineage such as $CD14^+$ and $CX3CR1^+$. Since both markers have to be expressed on each cell and many cells need to be analysed, we used flow cytometry, a technique that can analyse millions of cells at the single cell level for several markers simultaneously. The differentiation process produced both viable adherent and suspension cells separately. Figures 12 and 13 illustrate the flow cytometry plots demonstrating the expression of $CD14^+$ and $CX3CR1^+$ myeloid progenitors from the adherent and supernatant cells. In both figures the respective quadrants represent $CD14^+$ cells (Q1), $CD14^+$ and $CX3CR1^+$ cells (Q2), $CX3CR1^+$ cells (Q3), and the negative population (Q4). Figure 12A, shows the unstained supernatant cell controls, and clearly showed no expression of $CD14^+$ and $CX3CR1^+$ markers. The high background staining of the markers in their respective single quadrant is probably caused by autofluorescence an issue for flow cytometry analysis of stem cells. Similarly, autofluorescence can be detected in Figure 13A withing the single expression quadrants.

In the stained flow cytometry plots Figure 12B and 13B, the expression of both markers, $CD14^+$ and $CX3CR1^+$, is shown in progenitor cells with approximately 22.3% being double positive, while in Figure 13B, the dual expression is approximately 26.4%. Although there is a minor difference in expression levels, a higher expression in microglia progenitor cells overall would be preferable. The lower expression levels may be attributed to the timing of our flow experiment within the differentiation timeline. It is plausible that initiating marker expression analysis earlier in the process would have provided more insight. By incorporating regular marker expression checks using flow cytometry and maintaining lower cell confluency throughout the differentiation process, it is possible to enhance the proficiency and cell yield of microglia progenitor cells, similar to the results presented in the original article (46). Notably, even with lower expression levels of microglia progenitors compared to the original protocol, we were able to generate what we believe to be iPSC-derived microglia, as evidenced by the positive expression of multiple microglia makers, as shown in Figures 15 and 21.

Furthermore, the immunofluorescence stain performed at the end of the differentiation process, as depicted in Figure 15, revealed a robust and specific expression of IBA1 in differentiated cells. IBA1 is a commonly used intracellular microglia marker that can also stain for macrophages (21). Despite its non-specificity, the stain results showed a high expression of IBA1 in all our cells, indicating a promising outcome. Microglia cannot be identified and differentiated from other myeloid cells with one marker. For this reason, we have chosen the imaging platform Hyperion where positive and negative markers for lineage, differentiation and activation can be used simultaneously. It will be of great interest to further optimize the IMC protocol and adapt this powerful tool to the analysis of CSF cells in MS and other neurological diseases.

5.2 Characterisation of CSF cells

5.2.1 Establishment of an optimized IMC analysis pipeline for single cells from the CSF

The main objective of the project and the most challenging was the development of a technique to analyse single cells on the Hyperion, which is originally developed for tissue imaging. Firstly, we decided to test the cytospin to spin cells onto the slide. The deposition area of cells was about $28mm^2$, and suitable for high cell concentrations and we tested a range of concentrations from 250 cells/µl to 2500 cells/µl. For these cell numbers the cytospin worked as expected. However, the issue with CSF samples that contain much fewer cells became apparent as low cell concentration on the cytospin spread cells over a big area

that will be very expensive to analyse in the Hyperion which uses laser ablation. The usual cell concentration in CSF is 0-5 cells/µl, and between 5-50 cells/µl in MS patients, and using the cytospin for Hyperion analysis would not be cost-effective (13, 16). The area that needs to be ablated by the laser to acquire data is directly proportional to the ablation time, meaning a larger area requires a longer ablation time making it prohibitively costly. We concluded that cytospin is not an optimal method to fix rare cells on slides and proceeded to test other methods.

We tested drying small volumes of cell samples onto the microscope slide, with the use of a cell gasket to keep the cell deposition area contained to 7 mm^2 per well. This allowed us to use a small enough deposition area that would slightly counteract the very small cell concentration we were working with in our own samples. As shown in Figure 17 A) the drying of cells in PBS caused crystallization and may inhibit antibody binding or efficient ablation. PBS contains salts that, form crystalline structures when solid and the dried slide showed cells embedded in salt crystals. We solved this problem by changing the suspension medium to distilled H_2O, as this would not contain any salts and therefore should not present the same problem. In Figure 17 B) we can see that indeed, use of the dH_2O did solve this issue and we succeeded in collecting the cells in small areas of the slide suitable for fixation, staining and Hyperion analysis.

Fixation is an important step of many procedures and is known to affect epitope structure and therefore antibody binding depending on concentration and time the cells are left in paraformaldehyde. The adherence of cell to microscope slides by fixation showed no difference between 5 minutes of fixation and 10 minutes of fixation. To avoid epitope loss in longer fixations, we decided to use 5 minutes of fixation throughout our experiments. The test of fixing cells to the slides were performed with buffy coats that were fixed, red blood cells lysed and washed. However, the CSF cells and the iPSCs derived microglia samples were in proteomic stabilising solution that caused the cells to slide of the slide. After careful inspection of our biobanking protocols we noticed that our CSF and microglial cells had not been prepared in the same manner. All the cell types had proteomic stabilizer added to them for improved stabilization during freezing procedures, but the buffy coated cells and PBMCs had already had the stabilizer removed in a wash step using a thaw-lyse buffer while our CSF and microglial cells had not undergone this step. We postulated that this wash step could be the reason for the difference in fixation between the cell types, as the proteomic stabilizer contains methanol, which could interfere with the adherence of PFA fixed cells to the slide.

This shows the importance of biobanking samples in controlled manners for experiments. It is crucial to test fixation parameter further to find the most optimal parameters for the whole protocol from fixing the cells onto slides to antibody staining.

Antibody incubation time and temperature is known to affect antibody staining quality. The first Hyperion stain, shown in Figure 18 shows poor staining quality and required optimisation of antibody incubation time. The Intercalator stain was strong and we decided to try and reduce its incubation time while increasing our antibody incubation time. The results of these changes are visible in Figure 19 as this stain show more specific binding of our antibodies and less background staining. Even though these small changes led to substantial improvement, further optimisation is required to be able to analyse CSF cells with Hyperion.

5.2.2 Immunophenotyping of CSF cells with IMC

The reason for the channels chosen in Figures 20, 21 and 22 is that TMEM119 is the most specific microglia marker we have in our antibody panel and was specifically added to the panel because of this. While CD16 and MHC II both are markers that should be upregulated in activated microglia according to the literature (21, 52). CD3 was also shown because it's a T cell marker and should not be expressed on microglial cells. The characterisation of cells such as microglial requires a panel that includes both lineage negative and positive markers to identify immune cells and microglia. Our Hyperion panel contains 40 markers, but we were not able to test the whole Hyperion panel due to time limitations of the thesis. The panel should be able to efficiently detect microglia and immune cells and was developed in collaboration with experts in the microglia field. It will be very interesting to test the whole panel in future experiments.

Sample quality is another aspect that is important to consider. For CSF test we collected samples from the routine neurology laboratory. CSF samples should be clear and contain few red blood cells. However, our CSF samples were contaminated with red blood cells. Blood can sometimes contaminate CSF collection during the procedure. These red blood cells increase the difficulty of finding other immune cells when choosing areas to ablate and during analysis. In the future a step of red blood cell lysis should be added to the protocol when the CSF is red instead of clear.

Figure 20 shows a cell expressing TMEM119^{+}, CD16^{+}, and MHC II^{+} and indicates that this cell may be an activated microglia cell. While there is also a very small cell visible in the bottom left corner that is only showing specific expression of CD3^{+}, a T cell marker. Both the

size and the expression markers and the negative expression of CD3 are indicative of microglia. However, only staining with our full Hyperion panel will elucidate the difference between microglia and immune cells such as monocytes.

As mentioned earlier Iba1 is a common microglia marker, but not a specific one, as it can also stain for macrophages (21). And as such when we had performed the IF stain on our differentiated cells as shown in Figure 15, we could not be completely certain that the cells we had generated were iPSC-MG. In Figure 21 we show the results of the Hyperion stain of our differentiated cells, and as mentioned they show positive expression of multiple microglia markers, namely TMEM119, CD16 and MHC II. This in addition to the positive IBA1 stain performed earlier showed that there is a high certainty that the cells we generated were iPSC-MG. A noteworthy mention is that the TMEM119 is showing some extra background staining in this figure compared to the other channels and requires optimisation such as further titration.

The result shown in Figure 22 is as mentioned the CRL-3304 cell line we purchased, and this sample was the positive control for our microglia staining of CSF microglial cells and the iPSCs-differentiated microglial cells. These cells were positive for the $TMEM119^{+}$, $CD16^{+}$ and MHC II^{+} markers. Complex experiments require positive and negative controls and our approach shows that the choice of cell line and iPSCs derived microglia are appropriate positive controls while the PBMCs and buffy coats are negative controls for microglia and vice versa for immune cells of haematopoietic origin.

In Figure 23 & 24 we show different antibody stains in other channels than in the earlier figures pertaining to the main Hyperion experiment. We kept the microglia specific marker, TMEM119, and the T cell marker CD3, and analysed CD66b, CD45, and CD20 alongside them instead of CD16, and MHC II. The reasoning is that our negative control samples are PBMCs and buffy coated cells and, express typical immune lineage markers. CD45 being a leucocyte marker, CD66b being a neutrophil marker and CD20 being a B cell marker. The complexity of the technique requires that the panel is built up step by step in the optimisation phase. In addition, it is important to use the power of Hyperion by including negative and positive cell lineage markers and differentiation markers.

In Figure 23 we see no staining of $TMEM119^{+}$, and $CD66b^{+}$. We did not expect a positive stain for TMEM119 as is it a microglia specific marker, and few positive cells stained with CD66b. PBMCs, are collected by density centrifugation and eliminate most neutrophils.

Another potential reasoning for the small amount of specific staining visible in the sample is that the antibody staining did not perform as well as expected and following more optimisation, a higher percentage of $CD45^+$, $CD3^+$, and $CD20^+$ cells would be observed.

Figure 24 shows similarities with the sample in Figure 23, TMEM119 is not expected to be expressed on these cells. However, the immune markers CD45, CD3 and CD20 should have been detected in these immune cells and the results were unexpected as the buffy coat should contain leukocytes, T cells and B cells. We conclude that the procedure needs further optimisation for all the sample types included in this study. Figure 21 (C, G) shows clear expression of $CD66b^+$, showing that some of the cells visible are most likely neutrophils, which we definitively expect to find in the buffy coat.

5.3 Concluding remarks and future aspects

We have differentiated iPSCs into microglia and developed a novel technique for the analysis of single cells from CSF using high-dimensional imaging mass cytometry. The technique itself has required a high degree of optimisation and further steps are needed as well. Specifically, finding the optimal fixation time for multiple cell types while preserving epitopes is crucial. Expanding the antibody panel to include more microglia markers and immune markers of interest for MS specifically should be addressed. And reduction of background staining by antibody titration in all markers will optimise the signal to noise ratio and needs to be optimised further. As biomarkers found in CSF is of importance to MS diagnostic and therapy monitoring, we hope the development of this technique will help with discovery of biomarkers and further our understanding of the CNS immune architecture in MS and other neurodegenerative diseases. The technique opens the opportunity to investigate the CSF of patients with different neurological diseases at unprecedented resolution and characterise individual molecular signatures between them. The technique can elucidate mechanisms of pathogenesis in neuroinflammation and neurodegeneration since the CSF mirrors the process in the brain.

6. References

1. Bjornevik K, Cortese M, Healy BC, Kuhle J, Mina MJ, Leng Y, et al. Longitudinal analysis reveals high prevalence of Epstein-Barr virus associated with multiple sclerosis. Science. 2022;375(6578):296-301.

2. Filippi M, Bar-Or A, Piehl F, Preziosa P, Solari A, Vukusic S, et al. Multiple sclerosis. Nat Rev Dis Primers. 2018;4(1):43.
3. Baecher-Allan C, Kaskow BJ, Weiner HL. Multiple Sclerosis: Mechanisms and Immunotherapy. Neuron. 2018;97(4):742-68.
4. Lassmann H. Multiple Sclerosis Pathology. Cold Spring Harb Perspect Med. 2018;8(3).
5. Dendrou CA, Fugger L, Friese MA. Immunopathology of multiple sclerosis. Nat Rev Immunol. 2015;15(9):545-58.
6. Dutta R, Trapp BD. Mechanisms of neuronal dysfunction and degeneration in multiple sclerosis. Prog Neurobiol. 2011;93(1):1-12.
7. Kutzelnigg A, Lucchinetti CF, Stadelmann C, Bruck W, Rauschka H, Bergmann M, et al. Cortical demyelination and diffuse white matter injury in multiple sclerosis. Brain. 2005;128(Pt 11):2705-12.
8. Trapp BD, Nave KA. Multiple sclerosis: an immune or neurodegenerative disorder? Annu Rev Neurosci. 2008;31:247-69.
9. Kim W, Kim HJ. Multiple Sclerosis. Journal of the Korean Medical Association. 2009;52:665. Figure 2, Diagram representing the different types of multiple sclerosis. .
10. Baecher-Allan C, Kaskow BJ, Weiner HL. Multiple Sclerosis: Mechanisms and Immunotherapy. Neuron. 2018;97(4):742-68. Figure 4. Mechanisms in Progressive Multiple Sclerosis. .
11. Johanson CE, Duncan JA, 3rd, Klinge PM, Brinker T, Stopa EG, Silverberg GD. Multiplicity of cerebrospinal fluid functions: New challenges in health and disease. Cerebrospinal Fluid Res. 2008;5:10.
12. Redzic ZB, Preston JE, Duncan JA, Chodobski A, Szmydynger-Chodobska J. The choroid plexus-cerebrospinal fluid system: from development to aging. Curr Top Dev Biol. 2005;71:1-52.
13. Deisenhammer F, Zetterberg H, Fitzner B, Zettl UK. The Cerebrospinal Fluid in Multiple Sclerosis. Front Immunol. 2019;10:726.
14. Martin R, Bielekova B, Hohlfeld R, Utz U. Biomarkers in multiple sclerosis. Dis Markers. 2006;22(4):183-5.
15. Bielekova B, Martin R. Development of biomarkers in multiple sclerosis. Brain. 2004;127(Pt 7):1463-78.
16. Esaulova E, Cantoni C, Shchukina I, Zaitsev K, Bucelli RC, Wu GF, et al. Single-cell RNA-seq analysis of human CSF microglia and myeloid cells in neuroinflammation. Neurology - Neuroimmunology Neuroinflammation. 2020;7(4):e732.
17. Deisenhammer F, Zetterberg H, Fitzner B, Zettl UK. The Cerebrospinal Fluid in Multiple Sclerosis. Front Immunol. 2019;10:726. Figure 1, MS causes neuronal damage (demyelination, axon degeneration, synaptic loss) to the brain and spinal cord. Immune cells, pathological antibodies, adhesion molecules, cytokines, chemokines, and nucleic acids, which reflect inflammations in the CNS, are present in the CSF of the patients and can serve as biomarkers to support MS diagnosis and therapy.
18. Farhadian SF, Mehta SS, Zografou C, Robertson K, Price RW, Pappalardo J, et al. Single-cell RNA sequencing reveals microglia-like cells in cerebrospinal fluid during virologically suppressed HIV. JCI Insight. 2018;3(18):e121718.
19. Lannes N, Eppler E, Etemad S, Yotovski P, Filgueira L. Microglia at center stage: a comprehensive review about the versatile and unique residential macrophages of the central nervous system. Oncotarget. 2017;8(69):114393-413.
20. Muzio L, Viotti A, Martino G. Microglia in Neuroinflammation and Neurodegeneration: From Understanding to Therapy. Frontiers in Neuroscience. 2021;15.

21. Jurga AM, Paleczna M, Kuter KZ. Overview of General and Discriminating Markers of Differential Microglia Phenotypes. Front Cell Neurosci. 2020;14:198.
22. Lawson LJ, Perry VH, Dri P, Gordon S. Heterogeneity in the distribution and morphology of microglia in the normal adult mouse brain. Neuroscience. 1990;39(1):151-70.
23. Lawson LJ, Perry VH, Gordon S. Turnover of resident microglia in the normal adult mouse brain. Neuroscience. 1992;48(2):405-15.
24. Casano AM, Peri F. Microglia: multitasking specialists of the brain. Dev Cell. 2015;32(4):469-77.
25. Frost JL, Schafer DP. Microglia: Architects of the Developing Nervous System. Trends Cell Biol. 2016;26(8):587-97.
26. Sierra A, Encinas JM, Deudero JJ, Chancey JH, Enikolopov G, Overstreet-Wadiche LS, et al. Microglia shape adult hippocampal neurogenesis through apoptosis-coupled phagocytosis. Cell Stem Cell. 2010;7(4):483-95.
27. Dudvarski Stankovic N, Teodorczyk M, Ploen R, Zipp F, Schmidt MHH. Microglia–blood vessel interactions: a double-edged sword in brain pathologies. Acta Neuropathologica. 2016;131(3):347-63.
28. da Fonseca AC, Matias D, Garcia C, Amaral R, Geraldo LH, Freitas C, et al. The impact of microglial activation on blood-brain barrier in brain diseases. Front Cell Neurosci. 2014;8:362.
29. Gomez Perdiguero E, Klapproth K, Schulz C, Busch K, Azzoni E, Crozet L, et al. Tissue-resident macrophages originate from yolk-sac-derived erythro-myeloid progenitors. Nature. 2015;518(7540):547-51.
30. Nayak D, Roth TL, McGavern DB. Microglia development and function. Annu Rev Immunol. 2014;32:367-402.
31. Goldmann T, Wieghofer P, Jordão MJ, Prutek F, Hagemeyer N, Frenzel K, et al. Origin, fate and dynamics of macrophages at central nervous system interfaces. Nat Immunol. 2016;17(7):797-805.
32. Ajami B, Bennett JL, Krieger C, Tetzlaff W, Rossi FMV. Local self-renewal can sustain CNS microglia maintenance and function throughout adult life. Nature Neuroscience. 2007;10(12):1538-43.
33. Casano AM, Peri F. Microglia: multitasking specialists of the brain. Dev Cell. 2015;32(4):469-77. Figure 3, Schematic representation of microglial roles in the developing brain. Yellow and pink boxes indicate microglial roles during developmental stages and general immune-related functions, respectively.
34. Nakanishi M, Niidome T, Matsuda S, Akaike A, Kihara T, Sugimoto H. Microglia-derived interleukin-6 and leukaemia inhibitory factor promote astrocytic differentiation of neural stem/progenitor cells. Eur J Neurosci. 2007;25(3):649-58.
35. Shigemoto-Mogami Y, Hoshikawa K, Goldman JE, Sekino Y, Sato K. Microglia enhance neurogenesis and oligodendrogenesis in the early postnatal subventricular zone. J Neurosci. 2014;34(6):2231-43.
36. Luo C, Jian C, Liao Y, Huang Q, Wu Y, Liu X, et al. The role of microglia in multiple sclerosis. Neuropsychiatr Dis Treat. 2017;13:1661-7.
37. Miller E, Wachowicz B, Majsterek I. Advances in antioxidative therapy of multiple sclerosis. Curr Med Chem. 2013;20(37):4720-30.
38. Gray E, Thomas TL, Betmouni S, Scolding N, Love S. Elevated myeloperoxidase activity in white matter in multiple sclerosis. Neurosci Lett. 2008;444(2):195-8.
39. Fischer MT, Sharma R, Lim JL, Haider L, Frischer JM, Drexhage J, et al. NADPH oxidase expression in active multiple sclerosis lesions in relation to oxidative tissue damage and mitochondrial injury. Brain. 2012;135(Pt 3):886-99.

40. Neumann H, Kotter MR, Franklin RJ. Debris clearance by microglia: an essential link between degeneration and regeneration. Brain. 2009;132(Pt 2):288-95.
41. Lampron A, Larochelle A, Laflamme N, Préfontaine P, Plante MM, Sánchez MG, et al. Inefficient clearance of myelin debris by microglia impairs remyelinating processes. J Exp Med. 2015;212(4):481-95.
42. Voss EV, Škuljec J, Gudi V, Skripuletz T, Pul R, Trebst C, et al. Characterisation of microglia during de- and remyelination: can they create a repair promoting environment? Neurobiol Dis. 2012;45(1):519-28.
43. Liu G, David BT, Trawczynski M, Fessler RG. Advances in Pluripotent Stem Cells: History, Mechanisms, Technologies, and Applications. Stem Cell Rev Rep. 2020;16(1):3-32.
44. Takahashi K, Tanabe K, Ohnuki M, Narita M, Ichisaka T, Tomoda K, et al. Induction of Pluripotent Stem Cells from Adult Human Fibroblasts by Defined Factors. Cell. 2007;131(5):861-72.
45. Takahashi K, Yamanaka S. Induction of Pluripotent Stem Cells from Mouse Embryonic and Adult Fibroblast Cultures by Defined Factors. Cell. 2006;126(4):663-76.
46. Douvaras P, Sun B, Wang M, Kruglikov I, Lallos G, Zimmer M, et al. Directed Differentiation of Human Pluripotent Stem Cells to Microglia. Stem Cell Reports. 2017;8(6):1516-24.
47. Milosevic V. Different approaches to Imaging Mass Cytometry data analysis. Bioinformatics Advances. 2023;3.
48. Giesen C, Wang HA, Schapiro D, Zivanovic N, Jacobs A, Hattendorf B, et al. Highly multiplexed imaging of tumor tissues with subcellular resolution by mass cytometry. Nat Methods. 2014;11(4):417-22.
49. Milosevic V. Different approaches to Imaging Mass Cytometry data analysis. Bioinform Adv. 2023;3(1):vbad046. Figure 2, A schematic overview of the Imaging Mass Cytometry workflow.
50. Liang KX, Kristiansen CK, Mostafavi S, Vatne GH, Zantingh GA, Kianian A, et al. Disease-specific phenotypes in iPSC-derived neural stem cells with POLG mutations. EMBO Mol Med. 2020;12(10):e12146.
51. Douvaras P, Sun B, Wang M, Kruglikov I, Lallos G, Zimmer M, et al. Directed Differentiation of Human Pluripotent Stem Cells to Microglia. Stem Cell Reports. 2017;8(6):1516-24. Figure 1 A), Diagram depicting the major steps of the microglial differentiation protocol.
52. Ruan C, Elyaman W. A New Understanding of TMEM119 as a Marker of Microglia. Frontiers in Cellular Neuroscience. 2022;16.